SILICA-TITANIA COMPOSITES FOR WATER TREATMENT

By

DANIELLE JULIA LONDEREE

A THESIS PRESENTED TO THE GRADUATE SCHOOL
OF THE UNIVERSITY OF FLORIDA IN PARTIAL FULFILLMENT
OF THE REQUIREMENTS FOR THE DEGREE OF
MASTER OF ENGINEERING

UNIVERSITY OF FLORIDA

2002

ACKNOWLEDGMENTS

First of all, there is no way I could have accomplished this research without the help of my Lord and Savior. He has not only given me this opportunity, but also gave me peace and patience during the times of frustration. Second, without the help of my husband who kept me calm when my computer crashed several times, this work would not be done. He also stayed up with me many nights while I was writing and constantly gave me love and support.

I would like to thank Dr. David Mazyck for giving me the opportunity to work for him and learn from him. He has challenged me in many ways and I feel that I have learned more in the past two years of graduate school than the four years of undergrad. I thank him for patience and for purchasing the spectrophotometer. I thank Dr. Powers for allowing me to do an independent study with him. His excitement for research is contagious and motivational. I would also like to thank Dr. Paul Chadik and Dr. Chang-Yu Wu for giving advice during the research meetings and helping to provide answers for my many questions.

I thank the students in my research group and for those who have helped me get good data, specifically Matt Tennant (my mentor), Ameena Khan, Jennifer Hobbs, Christina Termaath, Jon Powell, Noworat Coowanitwong, and Julee MacKenzie.

TABLE OF CONTENTS

page

LIST OF TABLES

LIST OF FIGURES

Abstract of Thesis Presented to the Graduate School
of the University of Florida in Partial Fulfillment of the
Requirements for the Degree of Master of Engineering

SILICA-TITANIA COMPOSITES FOR WATER TREATMENT
By

Danielle Julia Londeree

December 2002

Chair: David Mazyck
Major Department: Environmental Engineering Sciences

Heterogeneous photocatalysis can be used for mineralizing organic dyes found in the effluent of textile dyeing operations. Incorporating the catalyst TiO_2 into an adsorbent material, such as silica, has many advantages over using a TiO_2 slurry for water purification. The goal of this research was twofold: 1) to produce a silica-titania composite using a sol-gel hydrolysis method that dopes the catalyst into the silica matrix during gelation and 2) to optimize the titania loading, curing temperature, and pore size of the material based upon maximizing its destruction and adsorption ability for textile dyes. The optimal titania loading found for reactive red dye was 30 wt% TiO_2. The optimal pore size and curing temperature found were 140 Å and 180^{o}C, respectively. These composites were also made into small cylindrical pellets and tested in a flow-through column to be used in a regenerative system. It was found that diffusivity was very important to efficiently regenerate the column using photocatalysis.

CHAPTER 1
INTRODUCTION

The textile industry's dyeing operations are of primary environmental concern, due to the variety of toxic chemicals (mostly solvents, surfactants, and acids) used in the dyeing of garments. According to the Environmental Protection Agency [EPA] (1997), chemicals such as methanol, methyl ethyl ketone, trichloroethylene, trimethylbenzene, and dyes such as basic green 4 and dispersive yellow 3 are released into the environment, either in the air phase or water phase. These contaminants can create large amounts of BOD (biochemical oxygen demand) and COD (chemical oxygen demand), as well as cause eutrophication and aquatic toxicity in effluent streams and natural water bodies. Color itself is increasingly being regulated, as there have been links to aquatic toxicity and lower DO (dissolved oxygen) values in receiving streams (EPA, 1996).

There are several chemical and physical methods of removal available for pre-release treatment, such as adsorption by activated carbon, biodegradation, and ozonation. Yet, dyes can be resistant to biodegradation and ozonation due to the large number of aromatic rings found in modern dyes (Sheng and Chi, 1993). Therefore, advanced oxidation processes are being considered as an emerging technology to handle large volumes of textile wastewater (Sauer et al., 2002; Wu et al., 1999). Of these processes, heterogeneous photocatalysis can be used for mineralization (complete conversion to CO_2 and H_2O) of several classes of organic compounds (including dyes), instead of transferring the pollutants from one phase to another (associated with carbon use).

Dyes can also be used as a surrogate for more toxic organic compounds in order to measure the photocatalytic ability of a system. For instance, the structure of methylene blue is similar to chloropromazine, an antipsychotic drug, and methylene blue destruction could be used to estimate the destruction of this drug. In this research, dyes were used to represent hard to degrade aromatic organic compounds in order to measure the performance of the silica-titania composites for water treatment.

In addition, NASA, with its construction of the International Space Station and plans for a Mars mission, requires a water recovery system that will minimize chemical additions and energy and provide water at a potable level. The water source to be treated will come mostly from grey water, including urine, humidity condensate, and wash water. NASA Document CTSD-ADV-245 also lists numerous organic compounds (many aromatic) that may be present in water in space flight (1998). The dyes used in this study are surrogates for those compounds that may be present in space flight for NASA.

There were two main objectives of this research. First, to develop a silica-titania composite by utilizing a sol-gel hydrolysis method and doping a highly efficient TiO_2 catalyst into the silica matrix during gelation. These composites could also be created into any shape and size, such as small cylindrical pellets to be used for a packed column. Second, the titania loading, curing temperature, and pore size of the composites were to be optimized based upon maximizing its destruction and adsorption ability for textile dyes. The result would be a combined adsorbent/photocatalyst that efficiently adsorbs contaminants into its pores for oxidation where the hydroxyl radicals would predominantly exist. It was hypothesized that a packed column of these composites made

into small pellets could create a regenerable system that could be used over and over again.

CHAPTER 2
LITERATURE REVIEW

2.1 Heterogeneous Photocatalysis

Advanced oxidation processes (AOPs) are considered to be an alternative water treatment technology for removing harmful compounds and microbes from public water supply, comparable with traditional practices such as activated carbon adsorption, air stripping, and chlorine disinfection. AOPs can not only disinfect the water from virulent microbes, but can also oxidize toxic heavy metals, organic pesticides and solvents, chlorinated compounds, and inorganic chemicals from the water without producing a waste stream unsuitable for disposal or consumption. For example, these processes can be used for chemical spill cleanup, treatment of industrial effluents, and wastewater treatment (Turchi and Ollis, 1990).

AOPs involve the generation of highly reactive oxidative species produced by several pathways, including reactions with H_2O_2 and O_3 with or without ultraviolet (UV) irradiation and heterogeneous photocatalysis. Heterogeneous photocatalysis entails the use of a solid photocatalyst (usually a semiconductor) in contact with either a liquid or gas, while homogeneous photocatalysis uses a catalyst of the same phase as the contaminated media. While UV use or an oxidant alone may yield partial degradation of a compound, the combined use of UV with an oxidant (with or without a photocatalyst) has been shown to yield complete mineralization of organic contaminants to carbon dioxide (Ollis et al., 1991).

The reactants in heterogeneous photocatalysis in water are naturally occurring species (such as oxygen, water molecules, and hydroxide ions (OH^-)) as compared to chemically supplied reactants (such as hydrogen peroxide and ozone) required for other AOPs. When the surface of the photocatalyst absorbs a specific amount of energy, an electron from the valence band jumps to the conduction band, thereby leaving a positive "hole" in the valence band. These electrons (e^-) and holes (h^+) may either recombine, releasing heat, or migrate to the surface of the catalyst. The reactive oxidative species are then generated from reactions with the electrons or holes on the surface (see Figure 2-1).

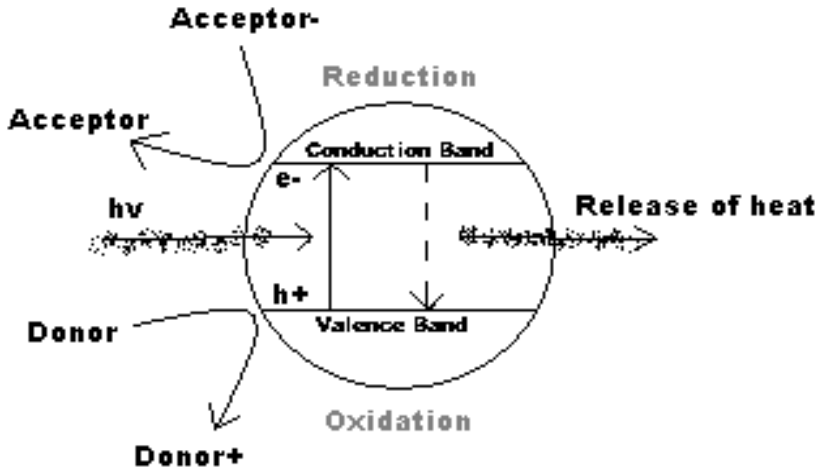

Figure 2-1. Schematic of oxidation and reduction occurring on the semiconductor surface.

The primary oxidizing species in water is the hydroxyl radical (*OH) (Turchi and Ollis, 1990). It is the most reactive of the oxidizing agents (see Table 2-1) and can be generated via several pathways:

$$H_2O + h^+ \longrightarrow {}^*OH + H^+ \qquad (1)$$

$$OH^- + h^+ \longrightarrow {}^*OH \qquad (2)$$

$$O_2 + 2H^+ + 2e^- \longrightarrow H_2O_2 \quad (3a)$$

$$H_2O_2 + e^- \longrightarrow {}^*OH + OH^- \quad (3b)$$

$$H_2O_2 \xrightarrow{hv} 2{}^*OH \quad (3c)$$

$$O_2 + e^- \longrightarrow O_2^- \quad (4a)$$

$$O_2^- + H_2O_2 \longrightarrow {}^*OH + OH^- + O_2 \quad (4b)$$

As can be seen from equations 1 – 4b, molecular oxygen plays a dual role in heterogeneous photocatalysis by 1) creating an oxidative species, the superoxide radical (O_2^-), and 2) acting as an electron acceptor to prevent the electrons and holes from recombining. These functions are very important in establishing an efficient photocatalytic system, for it has been shown that with an increase in oxygen concentration, there is a subsequent increase in the reaction rate of contaminant degradation (Gerischer and Heller, 1991). Similarly, hydrogen peroxide plays a parallel role.

Table 2-1. Oxidation power for various species relative to chlorine.

Species	**Relative Oxidation Power**
Hydroxyl radical	2.06
Singlet oxygen radical	1.78
Hydrogen peroxide	1.31
Perhydroxyl radical	1.25
Chlorine dioxide	1.15
Chlorine	1.00

Source: Elizardo, 1991.

Adsorption of compounds to the surface of the catalyst is also important in an efficient photocatalytic system. For instance, competition with other compounds can be

deleterious to the adsorption of specific contaminants on the catalyst surface. Chen et al. (1997) showed that the effect of inhibition due to competitive adsorption will hinder the degradation rate, especially in the presence of bicarbonate and phosphate. In addition, carbonate ions will also scavenge the hydroxyl radicals, thereby decreasing the destruction rate (Chen et al., 1997).

Another factor affecting adsorption is pH and the effect of pH is highly compound specific. For example, in the photocatalysis of textile dyes, a lower pH enhanced adsorption of Orange II (containing an anionic sulfonate group) to the catalyst surface, thereby increasing the rate of mineralization (Wu et al., 1999), while an alkaline pH increased adsorption and subsequent degradation of methylene blue (a cationic dye) (Houas et al., 2001). Sauer et al. (2000) also found similar relationships between adsorption and destruction of reactive dyes.

The photocatalytic mineralization of an organic compound begins with either reactions with hydroxyl radicals (or other less significant oxidizing species) or by direct oxidation with the holes on the surface of the catalyst. A hydroxyl radical “attacks” an organic compound by either removing an available hydrogen atom to form water or adding itself to any unsaturated carbon bonds (Grabner et al., 1991; Halmann, 1996; Hoffman et al., 1995; Hoigne, 1990; Mao et al., 1991, 1992, 1993). Mao et al. (1991, 1992, 1993) found that the rate of oxidation of organics correlated with the C-H bond strengths, proving that H atom abstraction by *OH may be a rate-limiting step. Consequently, from these primary reactions, an organic radical is formed (see Figure 2-2). The subsequent radical transformations and radical to radical interactions lead to an

array of intermediate products, eventually resulting in CO_2 and H_2O. For chlorinated compounds, HCl is also produced.

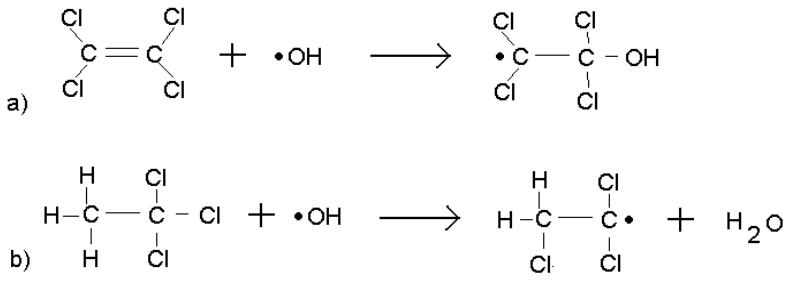

Figure 2-2. Example of hydroxyl radical attack a) on tetrachloroethylene by self-addition b) on 1,1,1-trichloroethane by hydrogen abstraction (notice chlorine shift in the radical) (adapted from Mao et al., 1991 and 1992).

There are several literature reviews available on the mineralization of particular classes of organic chemicals (Hoffman et al., 1995; Matthews, 1988; Ollis et al., 1991; Serpone, 1995). Blake (1995) and Halmann (1996) have compiled extensive surveys of this research and have also included sections on typical reactor designs and methods for catalyst improvement. Research has also been focused on the determination of the intermediate degradation pathways, for Mao et al. (1991 and 1992) has shown that the conditions of a system (pH, oxygen concentration, competition with other compounds) can affect the pathway a single compound can take towards complete mineralization.

2.2 Titanium Dioxide

Metal oxides are the most popular catalysts used for potable water and air treatment; of these, TiO_2 and ZnO have been the most researched and are considered the most efficient. Of these two, TiO_2 tends to be favored due to its stability in extreme conditions (low or high pH), insolubility, heat resistance, non-toxicity, and low cost. TiO_2

is also photostable as compared to ZnO which can undergo photocorrosion, decreasing the effective lifetime of the catalyst (Okamoto et al., 1985).

Titanium is the ninth most abundant element in the earth's crust and occurs in nature only in combination with other elements, such as with oxygen to form TiO_2 (US Geological Survey, 2002). Naturally occurring forms of titanium dioxide are usually combined with iron ($FeTiO_3$ or $FeO\text{-}TiO_2$) and contain other impurities. Therefore, the TiO_2 (titania) used as a photocatalyst is manufactured from synthetic means.

Of the commercially available titanium dioxides, Degussa's P25 seems to be the most researched for its photocatalytic ability in water (Halmann, 1996). Table 2-2 shows a few specific characteristics of P25. The product is produced from high-temperature flame hydrolysis of $TiCl_4$ in the presence of oxygen and hydrogen and is then steam treated to remove HCl, resulting in a 70:30 anatase to rutile phase TiO_2 (Degussa Technical Bulletin, 1990). The phase of TiO_2 is important since the anatase crystal form is considered the more photoreactive of the two (Tanaka et al., 1991). Figure 2-3 shows the crystal structures of the two phases. A difference in reactivity of the phases is attributed to 1) the more positive conduction band of the rutile phase, hindering molecular oxygen to act as an electron acceptor, and 2) the difference in surface properties between the two phases (Tanaka et al., 1991).

Table 2-2. Characteristics of Degussa P25 Titanium Dioxide

BET Surface Area	50 m^2/g
Average Primary Particle Size	21 nm
Band Gap: anatase, rutile	3.29 eV, 3.05 eV
Point of Zero Charge	pH 6.0

Source: adapted from Degussa Technical Bulletin (1990)

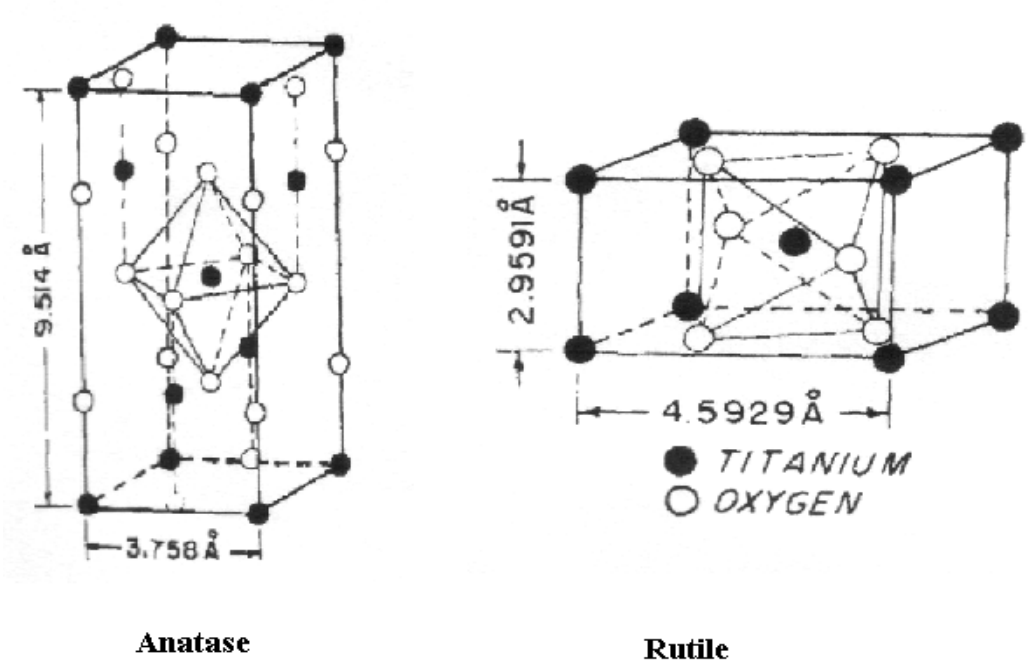

Figure 2-3. Diagram of anatase and rutile crystal structures (Millennium Chemical, 2002).

Crystal morphology, as well as a variety of other factors, can influence the activity of a catalyst. Surface area is known to affect the adsorption ability of the catalyst, as well as the available contact area for oxidation and reduction reactions. It would make sense that a catalyst with a large surface area would have an increased rate of reaction, but Tanaka et al. (1991) and Mills et al. (1994) showed that the destruction efficiencies of several different titanium dioxide samples were independent of surface area (within the range of 2.75 m^2/g to 177 m^2/g). Therefore, variables besides surface area may have a more influential role in the activity of a catalyst. These variables are crystal morphology, as well as crystallite size, prevention of electron-hole recombinations, zeta potential, and band gap energy (Okamoto et al., 1985; Palmisano and Sclafani, 1997; Suri et al., 1993; Tanaka et al, 1991; Zhang et al., 2001).

Tanaka et al. (1991) showed that the photocatalytic ability of a TiO_2 catalyst is foremost affected by the anatase content and secondarily affected by the size of the

crystal. For example, a photocatalyst containing larger crystals is more efficient than one with smaller crystals, even when both contain equal percentages of anatase. This could be due to the larger migration distance of the holes and electrons to the surface of the catalyst, thereby decreasing the possibility of recombination (Tanaka et al., 1991).

Modifications in the catalyst surface have also been investigated for prevention of electron-hole recombination. The addition of platinum and other transition metals have been successfully arrayed on the titanium dioxide surface (Abrahams et al., 1985; Okamoto et al., 1985; Martin et al., 1994; Suri et al., 1993). These metal additions have an optimum at low weight percentages (less than 5%), above which the metal actually hinders the photocatalytic ability.

The isoelectric point or point of zero charge (PZC) represents the pH at which an immersed solid oxide would have zero net charge, resulting in electrically equivalent concentrations of positive and negative complexes on the surface. At a pH above the PZC, interactions with cationic electron donors and acceptors will be favored; while anionic electron donors and acceptors will be favored at pH below the PZC.

The band gap is equal to the amount of energy required to activate the surface of the catalyst. A band gap of 3.29eV corresponds to a wavelength of 378 nm. Therefore, wavelengths below 378 nm (such as those emitted by UV light) would have the required energy to activate the anatase phase of TiO_2.

2.3 Reactor Design

A problem in the practical application of heterogeneous photocatalysis of environmental pollutants is the design of a reactor that will maximize photocatalytic efficiency while utilizing the least amount of energy. The simplest reactor configuration uses an aqueous suspension or slurry of the photocatalyst. Most photocatalysis studies

use a slurry system in preliminary testing to establish the feasibility of pollutant mineralization or microbe inactivation. For these systems, an optimum weight of TiO_2 per volume of solution (wt/vol) was found that yielded the most degradation for specific types of compounds at a specific light intensity. For instance, Goswami et al. (1993) found 0.1% (wt/vol) TiO_2 to be the optimum loading for most hydrocarbons and Block and Goswami (1995) found 0.01% (wt/vol) as the best for microbial destruction.

Although slurry systems are considered to be the most photocatalytically efficient, there is a dilemma to be addressed in the design of the reactor. Due to the extremely small size of the particles (between 0.1 – 30 nm, depending on the manufacturing source), there is a difficulty in recovering the catalyst from the purified water. This problem has directed research to investigate the use of catalyst supports.

There are many research groups that have examined the immobilization of photocatalysts on nonporous glass surfaces as a way of providing a backbone of support for the particles, while also allowing the penetration of light to activate the catalyst surface. Successful immobilization has been done on glass beads (Jackson et al., 1991; Serpone et al., 1986; Zhang et al., 1994) and on the inside surface of glass tubes (Al-Ekabi and Serpone, 1988; Matthews, 1988). The oxidation rates were usually lower with the immobilized catalysts than with free suspensions. The determinate factor was assumed to be the result of mass transfer limitations, for it was observed that as the flow rate increased, resulting in more efficient mixing, the oxidation rate likewise increased.

While these designs may have certain advantages, it is hypothesized that an efficient support for a catalyst would be a material with adsorption capability that would bring the contaminants into close contact with the catalyst surface (see Figure 2-4) where

the hydroxyl radicals predominantly exist (Turchi and Ollis, 1990). Indeed, there has been a reported increase in destruction efficiency when the reactants are brought into close contact with the surface of activated TiO_2 particles. This increase could be due to the greater concentration of the substrate around the catalyst surface due to adsorption interactions, for it has been proven that the highest efficiency of photocatalytic degradation of organic pollutants is observed at relatively high concentrations of reagents (Emeline et al., 2000).

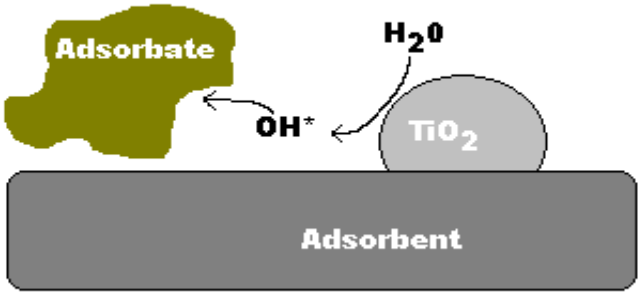

Figure 2-4. Simplified diagram of a catalyst support.

2.4 Catalyst Supports

Adsorbents researched as possible catalyst supports include activated carbon, silica gel, mordenite, alumina, zeolite, and aerogels (Takeda et al., 1995; Torimoto et al., 1996; Yoneyama and Torimoto, 2000). The highest decomposition rate for propyzamide (herbicide) was obtained with supports having medium adsorption strengths, such as silica and mordenite (Torimoto et al., 1996). With supports of too low (zeolite) and too high (activated carbon) adsorption strengths, no significant effect on the rate of destruction was found.

Yet, research has focused on the benefits of using activated carbon (AC) as a catalyst support versus other supports. Uchida et al. (1993) and Lu et al. (1999) found that while the oxidation rates of a specific compound were lower with the TiO_2 loaded AC, the complete mineralization rates were greater than with a plain slurry of TiO_2 or any other catalyst loaded support. They concluded that the lower oxidation rate can be attributed to the carbon blocking some of the photons of light from reaching the catalyst surface and the higher mineralization rate can be attributed to the high adsorptive ability of the carbon to adsorb the intermediate compounds that are being formed.

An additional benefit of TiO_2 coated carbon is its potential for in situ AC regeneration. Many water utilities use granular activated carbon (GAC) for the removal of organic compounds. However, after the absorbent is spent, removal of the carbon from the system is required for reactivation, disposal in a hazardous waste landfill, or incineration. While on-site thermal reactivation is an option for some utilities, it is not the most economical option for many. Therefore, research has been looking at optimizing both TiO_2-coated carbon's adsorption capability and its regeneration efficiency for the removal and subsequent oxidation of organic pollutants adsorbed on the spent carbon surface (Crittenden et al., 1993; Khan et al., 2002; Sheintuch and Matatov-Meytal, 1999).

While activated carbon has some benefits as a catalyst support, its use requires a reactor that efficiently exposes the catalyst surface to the photons of light. Since this may require mixing or fluidizing the particles, the inherent attrition can cause the catalyst to detach itself from the carbon (Lu et al., 1999). An additional problem is that the surface chemistry of a carbon may hinder effective coating (Khan et al, 2002). The various methods of activating carbon can create different functional groups on the surface, thus

affecting the properties a specific carbon will display. This can greatly affect the immobilization of a catalyst to the carbon surface.

Silica gels, on the other hand, have many advantages over activated carbon as a catalyst support. The transparency of silica allows the penetration of photons to the catalyst surface. This is extremely beneficial and allows for a fixed-bed reactor design that can be highly efficient in relation to input energy. Silica also has high mechanical strength, thermal stability, and can be synthetically formed into any shape, such as cylindrical pellets (Yamazaki et al., 2001) or fibers (Brinker and Scherer, 1990). In addition, silica is an adsorbent and is commonly used in chromatography columns for adsorption and the resulting separation of compounds in an aqueous sample. Furthermore, TiO_2 and SiO_2 can be chemically combined, enabling the formation of highly efficient photocatalysts. These TiO_2 - SiO_2 photocatalysts allow the placement of the catalyst on both external surfaces and internal surfaces within the porous silica matrix where pollutants are adsorbed.

Anderson and Bard (1995, 1997) found a strong synergy between silica and titania as a combined oxide. For substances that are easily adsorbed to the silica surface, a higher decomposition rate was found with TiO_2 - SiO_2 composites versus a plain TiO_2 slurry. The presence of an adsorbent was considered to promote efficiency by increasing the concentration of the substrate near the TiO_2 sites relative to the solution concentration. But for substrates that are not readily adsorbed to the surface of silica, the degradation rates were lower than compared to a slurry of pure TiO_2. However, when these rates were normalized to the TiO_2 content of the material, the TiO_2-SiO_2 material

demonstrated a more efficient use of the TiO_2 sites than for TiO_2 alone. The highest initial degradation rate was found with a 30/70 wt% TiO_2-SiO_2 composite.

Jung and Park (2000) also found 30 wt% titania (with gels prepared in a similar process to Anderson and Bard) to be the optimum in their studies for the mineralization of trichloroethylene. In addition, they concluded that the high porosity and large pore size of the silica facilitated the mass transfer of reactants, resulting in a higher rate of degradation than a plain slurry of Degussa P25.

Chun et al. (2001) used a different preparation method than Jung and Park (2000) and Anderson and Bard (1995) and still found 30 wt% TiO_2 to be an optimum. Chun et al. additionally showed, using two organic compounds with differing characteristics, that there is a strong correlation between adsorption of the compound on the mixed oxide surface and the destruction rate of that compound. In conclusion, silica-titania composites can be efficiently utilized in heterogeneous photocatalysis systems for the adsorption and subsequent destruction of unwanted compounds in an aqueous solution. In addition, a dosage of 30 wt% (equal to 12% on a weight per volume of silica precursor) was also found to be an optimum loading in this research (see Chapter 4) for the silica-titanium composites created using a sol-gel doping method (see Chapter 3).

2.5 Silica-Titania Composites

Silica is the most abundant oxide on the earth, yet despite this abundance, silica is predominantly made by synthetic means for its use in technological applications. Since synthetic silicas have a higher surface area than naturally occurring forms of silica, the synthetic silicas provide the best adsorption and catalyst support structure for heterogeneous photocatalysis. Although silica has a simple chemical formula (SiO_2), it can exist in a variety of forms, each with its own structural characteristics, as well as

chemical and physical properties. In general, SiO_2 is a SiO_4 tetrahedra, where each silica atom is bonded to four oxygen atoms and each oxygen atom is bound to two silica atoms.

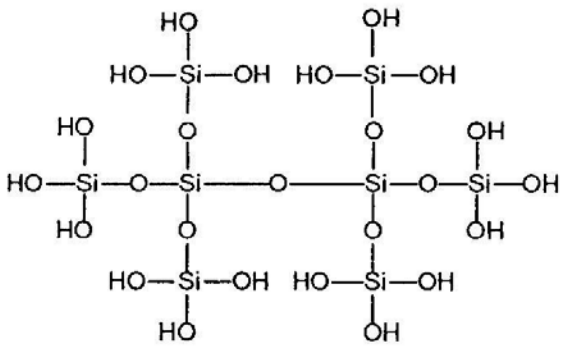

Figure 2-5. Linkages of SiO_2 tetrahedras (Hench and West, 1990).

There has been much research on the different preparation methods for creating a solid SiO_2-TiO_2 material with photocatalytic ability. The characteristics (e.g., pore size, surface charge, mechanical strength, and adsorption sites) of the final product are dependent on the synthesis conditions and the type of interaction between TiO_2 and SiO_2. There are two forms of interaction: physical forces of attraction (such as Van der Waals forces) and chemical bonding (creation of a Ti – O – Si bond). The physically supported TiO_2 on SiO_2 preparation methods have been the least researched, while the chemically bonded TiO_2 on SiO_2 methods (also called mixed oxides) have been thoroughly investigated (Gao and Wachs, 1999).

The most widely used methods of preparation (for details on these individual methods, see Appendix A) for creating mixed oxides are sol-gel hydrolysis and coprecipitation. Chemical vapor deposition, precipitation, and impregnation are the methods commonly used for creating supported oxides, yet there is evidence of Ti-O-Si bonds attaching the titania to the silica surface (Chun et al., 2001). A problem with supported oxides is the inconsistency in the coating from one batch to the next and the

nonuniformity of the coating due to the sensitivity of the procedure to its conditions (Hanprasopwattana et al., 1996; Lei et al., 1999). Another problem with any of these methods is the assurance of the formation of an anatase phase of TiO_2. Even though X-ray diffraction (XRD) can be used to determine the phase of TiO_2, the question remains whether the preparation method has formed the most efficient semiconductor particle, as compared to commercially available photocatalysts. For example, Liu and Cheng (1995) produced a TiO_2-SiO_2 mixed oxide using coprecipitation and found that the SiO_2 inhibits the growth of TiO_2 crystals, resulting in amorphous TiO_2 within the silica matrix.

A method of titania incorporation in silica has been devised to overcome both of these potential problems. This method uses sol-gel hydrolysis to create the silica matrix, then during gelation the solution is doped with the commercially available highly efficient Degussa P25 TiO_2. The silica network may either form around the titania particle and/or form a bond with the titania to secure its position in the matrix.

2.5.1 Sol-Gel Chemistry

A *sol* is a colloidal suspension of particles, while the term *gel* refers to the semi-rigid material formed when the colloidal particles link together in a liquid to form a network. Sol-gel precursors consist of metals or metalloids surrounded by various ligands, of which the most widely used are metal alkoxides (Mauritz, 2002). Aluminates, titanates, borates, and silicates are just some of the alkoxides that can be used to create a sol-gel. A gel that contains SiO_2 networks is given the term *silica gel*.

Hydrolysis and condensation. Gels derived from alkoxides form through hydrolysis reactions followed by condensation reactions (Equations 5-7). Generally speaking, hydrolysis replaces the alkoxide group with a hydrogen ion while condensation produces siloxane bonding (Si-O-Si) with the products of the reaction being water or

alcohol. As the number of siloxane bonds increases, the individual molecules join together to create a silica network. See Equations 5-7 (Mauritz, 2000).

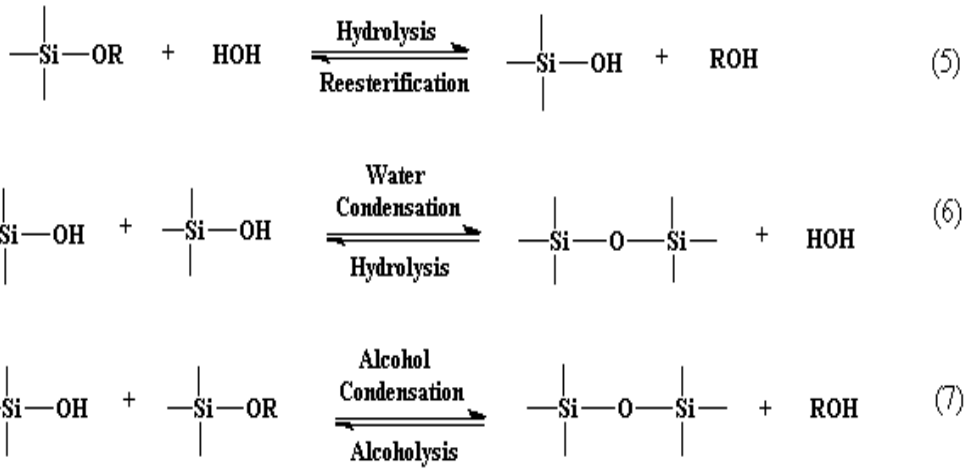

Gelation. After condensation reactions begin, gelation can occur (see Figure 2-6 for structure changes). Gelation is considered the growth period for the colloidal particles, which grow by polymerization or aggregation, depending on the conditions. Eventually, as the last links are made, the sol's viscosity increases to the point where the sol becomes a semi-rigid gel that consists of a network of pores filled with liquid.

Aging. Aging occurs after gelation. Here, terminal silanols re-orient themselves and react with each other to form additional network linkages. This results in shrinkage of the gel and forces the removal of some liquid from the pores. As the gel stiffens, "Ostwald ripening" occurs. This is the phenomenon whereby necks begin to form between primary particles causing the filling of small pores (see Figure 2-6 part c).

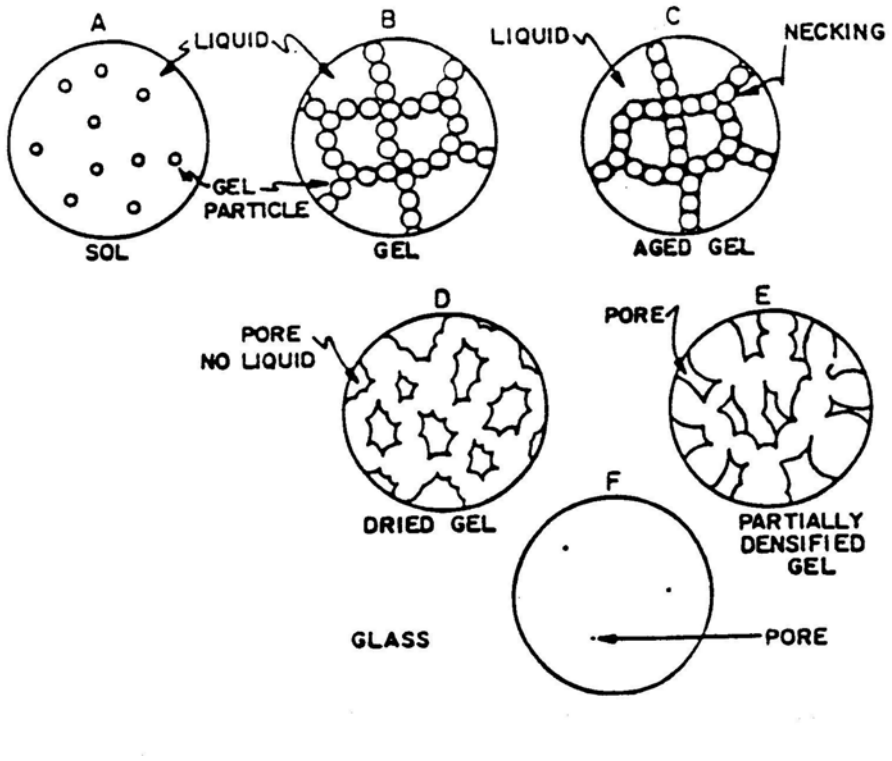

Figure 2-6. Structural changes during the sol-gel process (adapted from Hench and West, 1990)

Drying. The drying step involves the removal of the solvent from within the pores of the gel. This is very important in the determination of pore size. There are three types of gels characterized by the solvent removal process: xerogels, aerogels, and cryogels. As defined by Legrand (1998), a xerogel is obtained by evaporation of the liquid component at ambient pressure and temperatures below the critical temperature of the liquid; an aerogel is obtained from the evaporation of the liquid component above its critical temperature; and a cryogel is obtained from the freezing and subsequent sublimation of the liquid component. Aerogels have higher surface areas than xerogels and do not have a material volume loss due to shrinkage. Yet, because supercritically drying gels can be cumbrous and expensive, research has focused on making xerogels with similar

characteristics to aerogels. As far as water treatment is concerned, xerogels would be preferred over aerogels due to the higher mechanical strength of the xerogel.

Curing. Calcination or curing is the final heat treatment step in producing a mechanically strong gel. This thermal treatment also affects several characteristics of the silica gel. With increased heat treatment, the BET (Brunauer, Emmett, and Teller equation) surface area will decrease due to sintering (Papirer, 2000) and the dehydration (around 180-200^{o} C) and subsequent dehydroxylation (above 200^{o} C) of the surface of the silica, resulting in the formation of siloxane bridges (Holysz, 1998). The final product resulting from all these steps (hydrolysis, condensation, gelation, aging, drying, curing) is a gel containing a relatively monodisperse pore size and displaying specific characteristics associated with the conditions it experienced during processing.

Effect of catalyst. The two alkoxides most often used are tetramethoxysilane (TMOS) and tetraethoxysilane (TEOS). TMOS has the advantage of rapid hydrolysis under a variety of conditions, but the toxic methanol produced can be hazardous to the eyes and lungs. Conversely, TEOS is hydrolysis rate limited (Brinker and Scherer, 1990), but produces less toxic ethanol during the reaction. To increase the hydrolysis reaction rate of TEOS, an acid or base can be added as a catalyst. However, the nature and concentration of the catalyst will affect the characteristics of the gel. For example, the addition of hydrofluoric acid will rapidly increase the rate of gelation as well as increase the pore size (Powers, 1998).

Other important parameters to consider in the production of a gel are H_2O to Si molar ratio (called the "R" factor) and the aging and drying schedules. A high R ratio will promote more rapid hydrolysis, for the concentration of water affects the rate of

hydrolysis. The drying time and temperature also affect the pore size of the gel as well as the shape of the gel. For example, the longer the time to dry, the more Ostwald ripening occurs and the less likely the gel will crack, thereby producing a larger pore size than a gel of the same composition dried in short period of time (less than 48 hours). In summary, there are many parameters in the production of a gel that will greatly affect the final product's characteristics. It is these differences in silicas produced by various preparation methods that make the comparison of data found in the literature a very difficult process.

2.5.2 Surface Chemistry and Adsorption Characteristics

The surface of silica consists of two types of functional groups: silanol groups (Si – O – H) and siloxane groups (Si – O – Si). The silanol groups are the locale of activity for any process taking place on the surface, while siloxane sites are considered nonreactive (Unger, 1979). Porous amorphous silica contains three types of silanols on its surface: isolated, geminal, and vicinal (or associated). Figure 2-7 shows the distinction between these groups. The unequal distribution of the silanols in the sililca matrix, resulting from irregular packing of macromolecules as well as incomplete condensation, results in a heterogeneous surface (non-uniformity in the dispersion of silanol groups) for synthesized silica (El Shafei, 2000).

The various silanols can have different adsorption activity and current knowledge indicates that the isolated silanols are the more reactive species (Nawrocki, 1997; El Shafei, 2000). With increasing temperature of heat treatment, the silica surface becomes hydrophobic due to the condensation of surface hydroxyls (dehydroxylation) and the formation of siloxane bridges (see Figure 2-8). This increases the ratio of isolated sites versus other silanol groups on the surface and therefore increases adsorption.

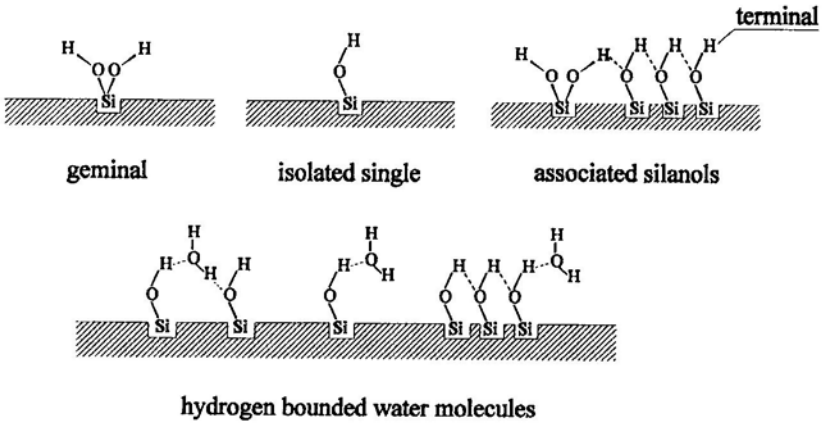

Figure 2-7. Silanol groups on the silica surface (Legrand, 1998).

At temperatures up to 450°C, the removal of the hydroxyl groups does not result in visible changes in structure, density, or specific surface area of the silica because the rehydroxylation makes it possible to return to the initial state (Davydov, 2000). Rehydroxylation of the silica surface by exposure to water vapor is reversible up to 600°C. At temperatures above this, the rehydroxylation becomes a slow process or remains incomplete (Unger et al., 2000). Also, there is a decrease in surface area as a result of sintering at temperatures above 500°C (Persello, 2000).

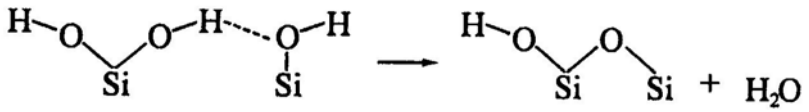

Figure 2-8. Representation of dehydroxylation (Burneau and Gallas, 1998).

Pore size can be affected by the heat treatment of the silica, but is also a function of the manufacturing process. The effect of pore size on adsorption is dependent on the compound's characteristics, such as molecule size, shape, and functional groups (Dabrowski, 2001; Goworek et al., 1997; Goworek et al., 1999). In general, the smaller the pore, the larger the surface area and the larger the capacity for adsorption of

contaminants. Yet, Goworek et al. (1997) found that some compounds may be hindered by a narrow pore size due to steric forces. Therefore, the adsorption ability for that particular compound would be higher in a silica with larger pores.

Adsorption on silica surfaces is primarily due to ion interactions and hydrogen bonding with the silanol groups. Therefore, the adsorption kinetics in relation to these silanols is greatly dependent on the pH. Silica's point of zero charge ranges between 2 and 3 (Papirer, 2000; Persello, 2000). At a pH less than the PZC, the surface has a positive charge due to the formation of $Si\text{-}OH_2^+$. At a pH above the PZC, the surface of the silica has a negative charge due to the deprotonation of the silanol group resulting in $Si\text{-}O^-$. As the pH approaches 7, the $Si\text{-}O^-$ sites become significant (the pKa for SiOH = $SiO^- + H^+$ is 7) (Cox, 1993). These $Si\text{-}O^-$ sites readily react with cations in solution and an increase in pH would greatly increase the adsorption of these compounds (Kinniburgh and Jackson, 1981). For nonionic compounds in solution, adsorption can occur at the silanol groups by hydrogen bonding or by Van der Waals forces. For anionic compounds, there may be some adsorption at a pH above the PZC of silica, but it would be occurring at the TiO_2 surface because it is positively charged at $pH < 6.0$. One factor to consider when adjusting pH in order to achieve the highest adsorption onto silica-titania composites is the dissolution of silica at a pH greater than 9 (Iler, 1979). In order to create a long-lasting photocatalytic composite, the dissolution of silica would need to be avoided.

CHAPTER 3
MATERIALS AND METHODS

3.1 Silica-Titania Composites

The silica-titania composites were made by a sol-gel method (Powers, 1998) using nitric acid and hydrofluoric acid as catalysts to increase the hydrolysis and condensation rates, thereby decreasing the gelation time. The basic formula used to create gels with a pore size of roughly 140 Å is as follows: 25 mL water, 50 mL ethanol, 35 mL TEOS (tetraethylorthsilicate), 4 mL nitric acid (1N), and 4 mL HF (3%). TEOS was used in place of TMOS (tetramethylorthosilicate) because it produces less toxic ethanol instead of highly toxic methanol that would be created by reactions with TMOS. Varying the volume of hydrofluoric acid allowed the manipulation of the pore size. Decreasing the volume to 1 mL HF resulted in 30 Å pores, while increasing it to 8 mL resulted in 320 Å pores.

The chemicals (reagent grade from Fisher) were added individually, in no particular order, to a polymethylpentene container. A magnetic stir plate provided sufficient mixing. The solution was allowed to mix until gelation occurred (2 hours for 140 Å gel). During this time, a known mass of Degussa P25 was added to the batch and the percentage of titania recorded is given as a percent by volume of silica precursor. After gelation, the lid was put on, preventing any air exposure in order to protect against premature evaporation. Next, it was aged at room temperature for two days, then at 65^{o} C for two days. After aging, the gel was removed from the container, rinsed with deionized water to remove any residual acid or ethanol, and placed in a Teflon container for the

next series of heat treatments. A small hole in the lid of the container allowed slow and uniform drying of the gel. It was then placed in an oven and the temperature was ramped from room temperature to 103^{o} C (2^{o}/min) and kept constant for 18 hours, resulting in the vaporization of liquid solution within the silica network. Next, the temperature was ramped to 180^{o} C (2^{o}/min) to remove any physically adsorbed water. It was kept constant for 6 hours and then was slowly decreased back to room temperature over a 90 minute period. These gels were powdered and sieved through 325 mesh to be used for batch performance studies.

The titania-doped pellets were made in a similar fashion, except the solution (including the P25) was pipeted into polystyrene 96-well assay plates before gelation. The volume added to each well was approximately 0.3 mL. The plates were then covered with lids and wrapped in foil to prevent premature evaporation. The same aging and drying schedule as previously discussed was used, but before the drying step, the pellets were removed from their plates and placed in a Teflon container. The resultant size of an individual cylindrical pellet after drying was approximately 5 mm in length with a diameter of 3 mm. These pellets were used in column performance studies.

3.2 Batch Performance Studies

The batch performance studies were done to determine an optimal titania loading, curing temperature, and pore size that is efficient for both adsorption and destruction of contaminants. The powdered gels were compared based upon destruction (removal of color) of reactive red dye (RR) from Sigma-Aldrich and adsorption of crystal violet dye (CV) from Fisher. All dye solutions were made with nanopure water. The destruction studies were performed as follows: 30 mg of gel was added to 100 mL of a 10 mg/L RR solution buffered with 200 mg/L of sodium bicarbonate in a 125 mL Erlenmeyer flask.

Then pH adjustments were made with sodium hydroxide or nitric acid. The flask opening was then covered with parafilm to maintain a closed system with a limited amount of dissolved oxygen (DO). In a system designed for NASA, oxygen would be a limiting factor due to the problem of continually supplying oxygen for water treatment for long duration space flight. The flasks were placed within a box containing four magnetic mixers relatively equidistant from a single 4-Watt UV lamp. The UV exposure time was two hours and the percent destruction was calculated by comparing the initial and final absorbance readings using a Hach DR/4000U (Loveland, Colorado) Spectrophotometer at RR's peak absorption wavelength of 538 nm. The spectrophotometer gave a linear response across the concentration range for each dye. The UV intensity (mW/ cm^2) was varied by changing the position of the mixers in regard to the lamp and by the use of additional lamps. UV intensity (wavelengths between 320 to 380 nm) was measured with a VWR Ultraviolet Light Meter (Atlanta, GA). Each mixer was placed where the desired UV intensity was achieved at the mixer's center.

The adsorption studies were performed as follows: 30 mg of gel was added to 100 mL of 10 mg/L CV solution with no bicarbonate added. The studies were conducted at a pH of 4, using nitric acid and sodium hydroxide for the pH adjustments. The flasks were covered with parafilm and placed in a box with no penetration of light and allowed to mix for 24 hours. The percent adsorbed was calculated from the absorbance reading at a wavelength of 590 nm.

The BET (Brunauer, Emmett, and Teller equation) surface area and pore volume analysis was performed on a Quantachrome NOVA 1200 Gas Sorption Analyzer (Boynton Beach, FL). The powdered samples were outgassed at 110^{o} C for

approximately 24 hours and analyzed using nitrogen adsorption isotherms. The average pore size was calculated by dividing the pore volume by the surface area. Pore size distribution curves were also attained and coincided with the calculated pore size.

XRD (X-ray diffraction) analysis was performed on cured gels to determine the phase of titania, anatase or rutile. These gels were cured at temperatures up to 800^{o} C as an additional curing step after the regular drying schedule. The analysis was performed on a APD 3720 from Philips Analytical (Almelo, Netherlands). The reflections of the two crystalline TiO_2 phases, anatase ($2\theta = 25.3$) and rutile ($2\theta = 27.4$), were taken from Grieken et al. (2002).

3.3 Column Performance Studies

The purpose of these studies was to show the performance of the pellets in a regenerative system, which places equal significance on the adsorption of a contaminant as well as the feasibility of the contaminant to be mineralized. A cylindrical column (6 inches in length, 0.5 inch diameter) with a porous frit was filled with 10 mL of pellets. The column setup is shown in Figure 3-1. A CV dye solution of 2 mg/L was pumped through the column until the effluent concentration equaled the influent concentration. Then the CV pump was turned off and the deionized water and UV light was turned on (flux = 1.1 mW/cm^2) for a set time (e.g., one hour). During this regeneration time, the water was pumped through the column to provide the reactants (O_2, H_2O) required for photocatalysis. After the regeneration time, the CV pump was turned back on. This cycle was continued several times for separate packed columns of 140 Å gels and 30 Å pellets, both loaded with 12% TiO_2. The flowrate for both the deionized water and CV dye was 8 mL/min.

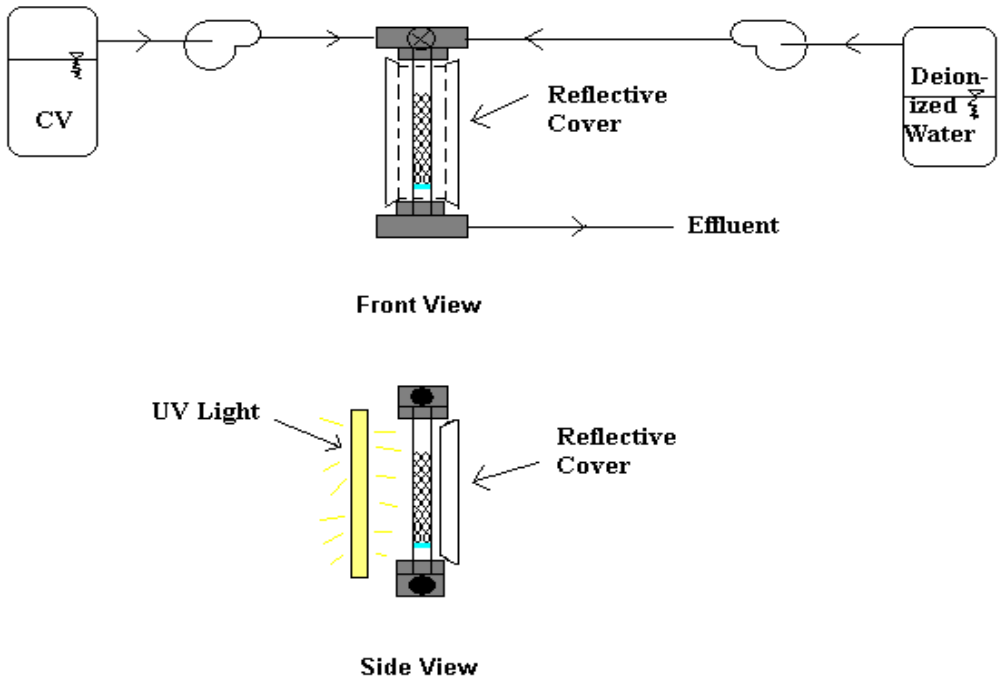

Figure 3-1. Column setup.

CHAPTER 4
RESULTS AND DISCUSSION

4.1 Dye Comparison

In order to accurately measure the photocatalytic ability of the silica-titania (SiO_2 – TiO_2) composites, it was important to choose a dye that displayed little or no photolytic behavior, i.e. change in absorbance as a response to UV light exposure alone. The following four dyes were examined in order to determine the most suitable dye for the studies herein: malachite green (MG), methylene blue (MB), crystal violet (CV), and reactive red (RR). See Appendix B for structures of these dyes.

Using a spectrophotometer, each dye was scanned at a range of 290 nm to 800 nm in order to find each dye's peak absorbance wavelength. A summary of the peak wavelengths is shown in Table 4-1. The absorbance measured at this peak wavelength was used for comparing initial and final readings.

Table 4-1. Peak absorbance wavelengths.

Dye	Peak Wavelength
MG	619 nm
MB	656 nm
CV	590 nm
RR	538 nm

A 100 mL solution of each dye (10 mg/L) was prepared in a 125 mL Erlenmeyer flask and exposed to three different intensities of UV light for two hours. The findings are presented in Figure 4-1. Each dye experienced a change in absorbance of less than 5% at each flux, except for crystal violet, which experienced a 19% change at a flux of 1.1

mW/cm^2. Based upon this undesirable change, crystal violet was excluded for future destruction studies.

Subsequently, the remaining dyes were evaluated for photolysis at various concentrations (0.5 mg/L to 10 mg/L). At 0.5 mg/L, there was a 98% and 20% change between the initial absorbance readings for MB and MG respectively, compared to their final readings after two hours of UV exposure (0.45 mW/cm^2) (Figure 4-2). Large discrepancies were also observed at 1 mg/L and 2 mg/L. Therefore, MB and MG were eliminated as viable candidates to investigate the photocatalytic ability of the composites. For RR (see Figure 4-3), the largest change in absorbance was only 13% at a flux of 1.1 mW/cm^2, the highest flux achievable. Thus, RR was chosen for the photocatalysis studies. The amount of photolysis was not subtracted from the results of the destruction studies.

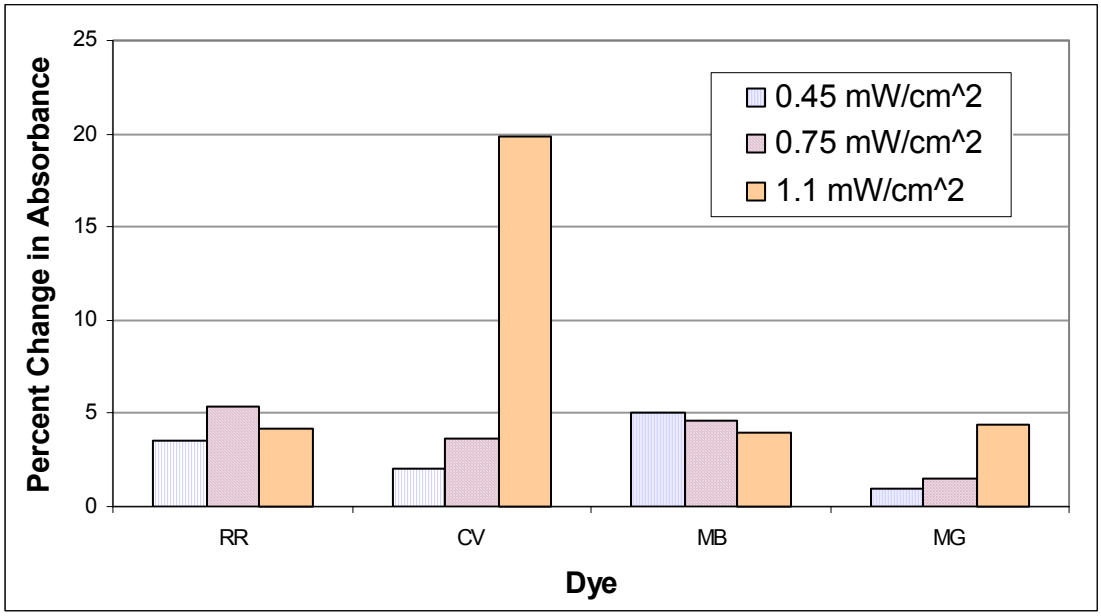

Figure 4-1. Photolysis of dyes as a function of UV flux for 2 hours of exposure.

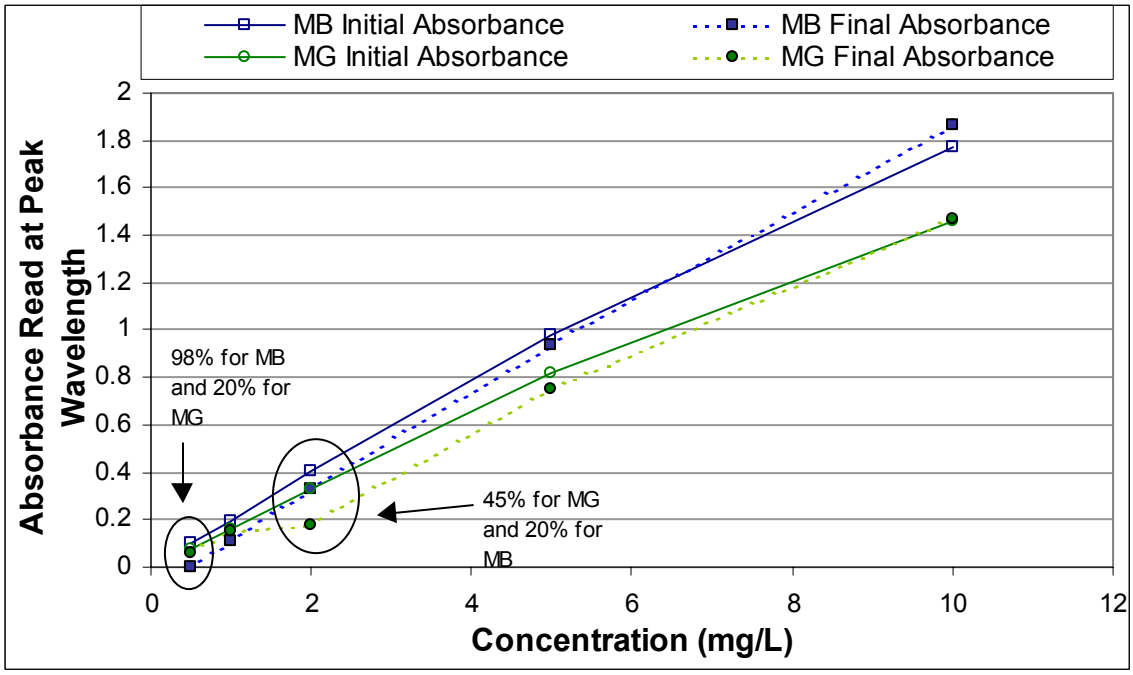

Figure 4-2. Photolysis of MB and MG (2 hours UV exposure at 0.45 mW/cm^2) as a function of initial dye concentration.

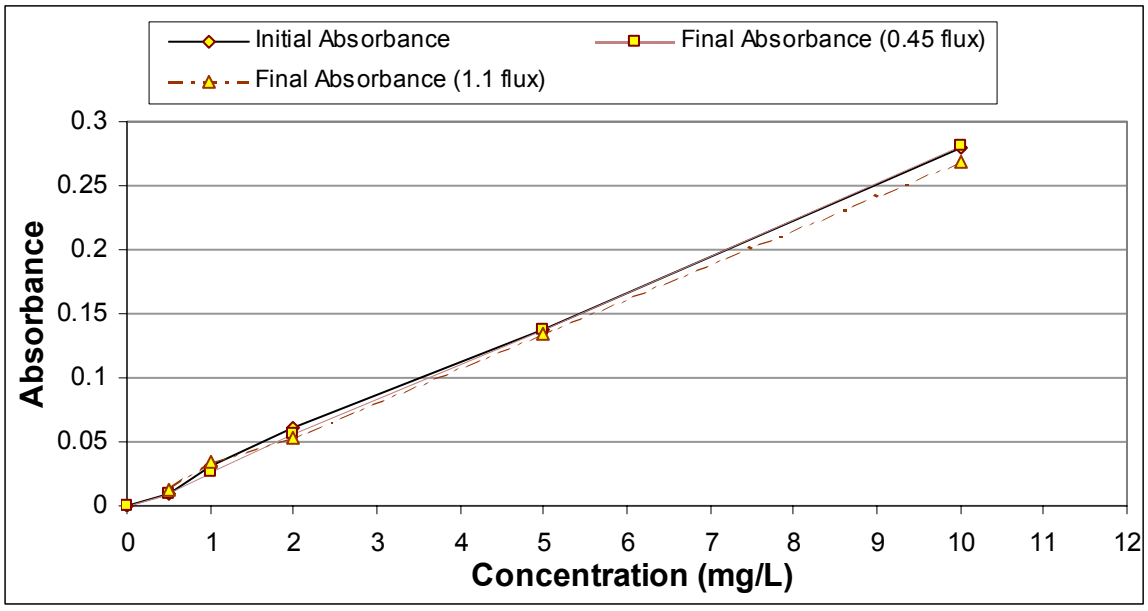

Figure 4-3. Photolysis of RR (2 hours UV exposure) as a function of initial dye concentration and flux.

Besides photolysis, pH can also affect a dye's peak absorption wavelength. Therefore, RR solutions of 10 mg/L were prepared at different pHs and compared before and after UV exposure. The change in absorbance (at 538 nm) as a function of pH is shown in Figure 4-4. At a pH above 8, there was a decrease in absorbance along with a slight visible change of color from a dark pink to a red. Figure 4-5 displays a section of the spectrophotometer scan and shows the changes that occur at an alkaline pH. At a pH of 7, the maximum peak wavelength is 538 nm. At a pH of 9.5, the highest peak occurs at both 514 nm, as well as 538 nm. After two hours of UV exposure, the max peak returns back to 538 nm. Also noticeable at pH 9.5 is a slight downshift in the curve after UV exposure. Therefore, the pH was kept below 8 for comparison studies of gels to ensure accurate measurements of destruction ability.

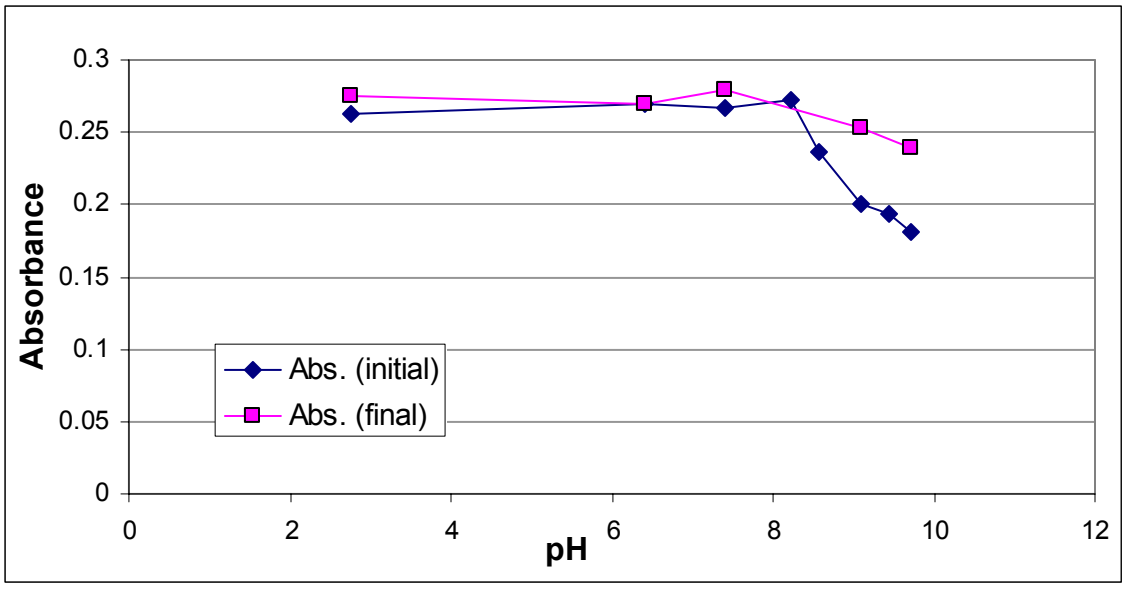

Figure 4-4. Change in absorbance of RR at 538 nm as a function of pH.

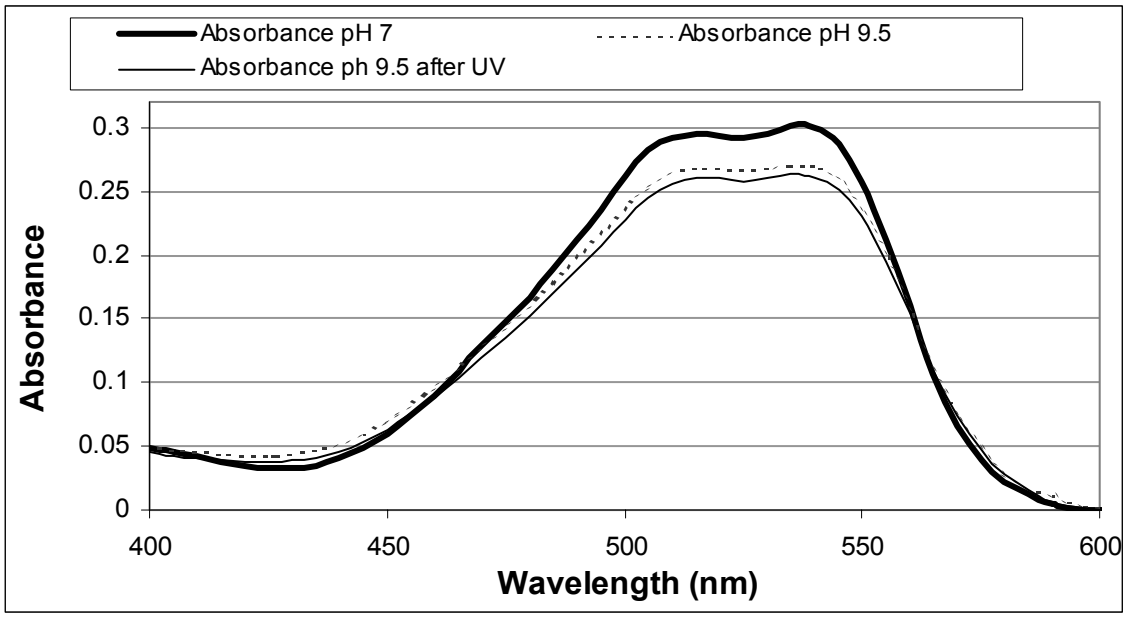

Figure 4-5. Spectrophotometer scan of 10 mg/L RR as a function of pH, before and after UV exposure.

4.2 Optimization of Gels

4.2.1 Titania Loading

In order to determine the optimal titania loading, 14 gels (140 Å) of varied TiO_2 loadings (from 0.77% to 40%) were created. The desired optimal loading would be found as the composite having the highest rate of destruction for RR. These gels were performance tested at three UV intensities for the destruction of RR (10 mg/L) and the results are displayed in Figure 4-6. There is a definite plateau where the percent destruction remains constant, even with the addition of more TiO_2. It appears that this plateau occurs at lower TiO_2 percentages with higher UV intensities. For 1.1 mW/cm^2, the plateau occurs at 5% TiO_2 and it occurs at 10% for 0.75 mW/cm^2. At the lowest UV intensity, the destruction levels off at 12%. These results were triplicated and the error bars are included in the figure.

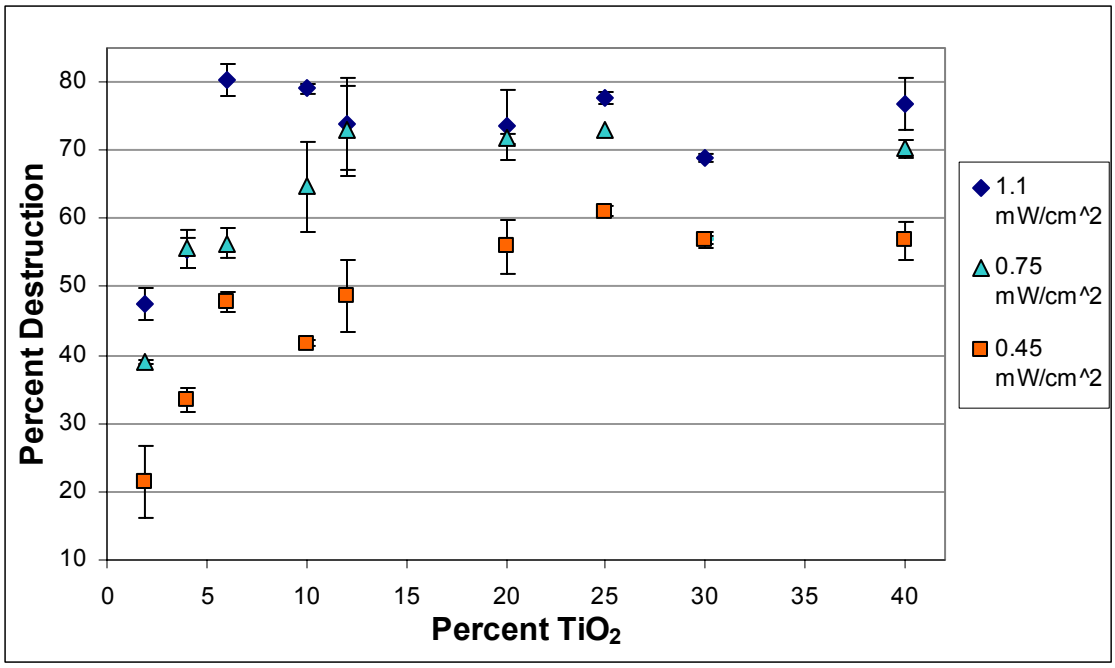

Figure 4-6. Destruction of RR (pH 7.6) after 2 hours UV exposure versus TiO_2 loading as a function of flux.

The plateau can be explained by the TiO_2 is agglomerating in solution during gel preparation, which was visually observed with TiO_2 loadings greater than 8%, and therefore is decreasing the effective surface area of titania available for excitation and/or oxidation and reduction reactions on its surface. The 12% optimal loading (wt/vol precursor) at the lowest energy is approximately equal to 30 wt%, which was found to be an optimum for destruction of organic compounds with other methods of producing silica-titania composites (Jung and Park, 2000; Chun et al., 2001; Anderson and Bard, 1995).

The structure of RR includes sodium sulfonate groups that would make the compound anionic when the sodium disassociates as the compound dissolves. Therefore, the effect of pH on adsorption and destruction of RR was also investigated. It was observed that at a pH range of 3 to 10, there was no adsorption of RR dye to the silica-

titania gels. Thus, the color disappearance of the dye can be directly attributed to photocatalysis with a minimal amount due to photolysis.

The effect of pH on the destruction of RR is shown in Figure 4-7. It was observed that acidic conditions enhanced the photocatalytic destruction of RR and it was initially hypothesized that this was due to the TiO_2 having a positive charge at pH 3, therefore, the amount of RR adsorption that would occur on pure TiO_2 at low pH would increase the destruction rate.

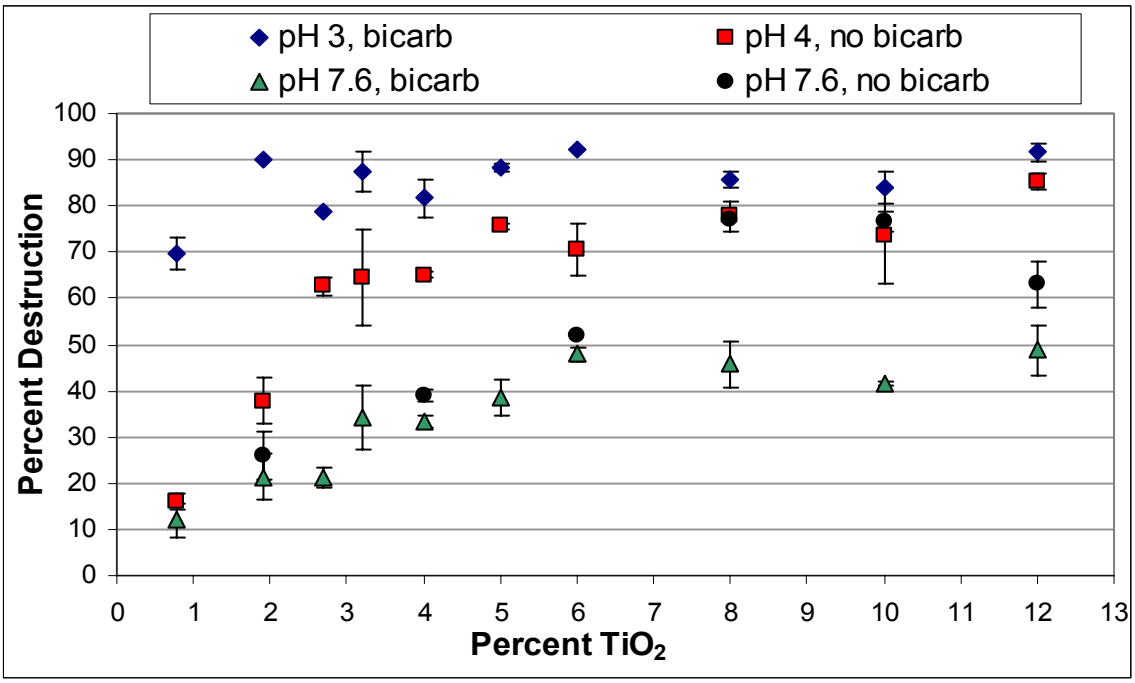

Figure 4-7. Destruction of RR (10 mg/L) after 2 hours UV exposure (0.45 mW/cm^2) versus TiO_2 loading as a function of pH.

Yet, when a slurry of titania was tested for destruction and adsorption at a range of pHs, the results were contrary to what was hypothesized (Figure 4-8). While the adsorption onto the titania surface may have slightly increased at a lower pH, the level of total removal (destruction and adsorption) did not change. It is then presumable that at a pH greater than 6, the silica surface becomes more concentrated with SiO^- groups, thus

repelling RR. As the pH approaches 3, the silica has less of a negative charge and would allow the penetration of RR into the pores. Hence, acidic conditions would increase the ability of RR to get within the vicinity of the titania.

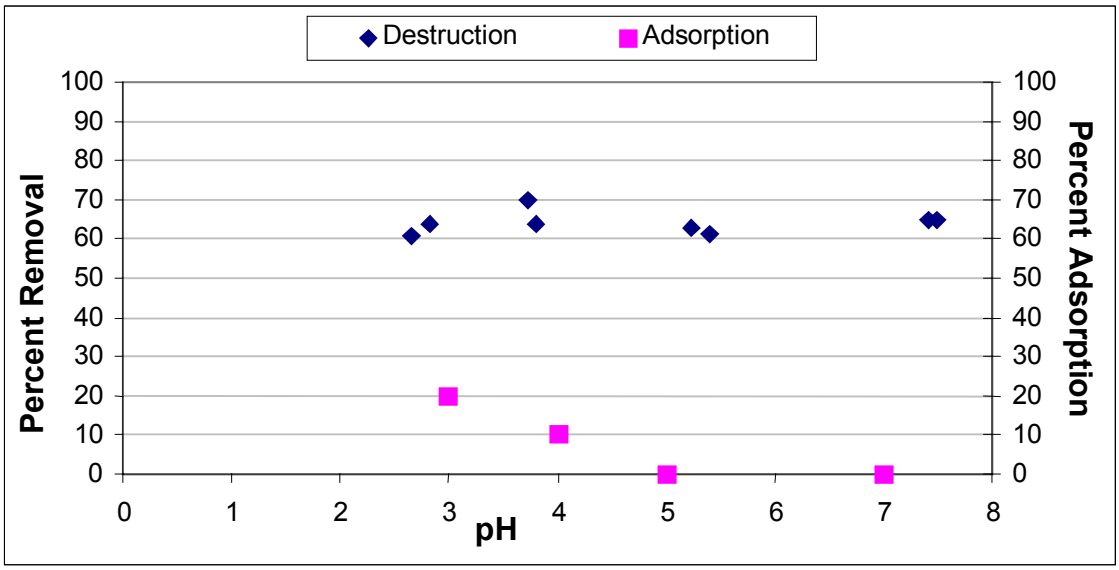

Figure 4-8. Destruction of RR (10 mg/L) after 1 hour UV with TiO_2 slurry at various pHs.

Grey water contains many sulfates, phosphates, and salts that may inhibit the destruction of unwanted compounds (Chen et al., 1997). The addition of sodium bicarbonate allows one to see the performance of the silica-titania composites in a realistic feed stream. In Figure 4-7, it is also interesting to notice the affect of bicarbonate on the destruction efficiency. There is little increase in destruction (with no bicarbonate) at a pH of 7.6 within a range of 0.77% to 6% TiO_2. At a larger TiO_2 percentage, the difference becomes very noticeable. However, Figure 4-9 shows that the increase in destruction without bicarbonate present is only seen within a certain range of TiO_2 loading (8% to 12%).

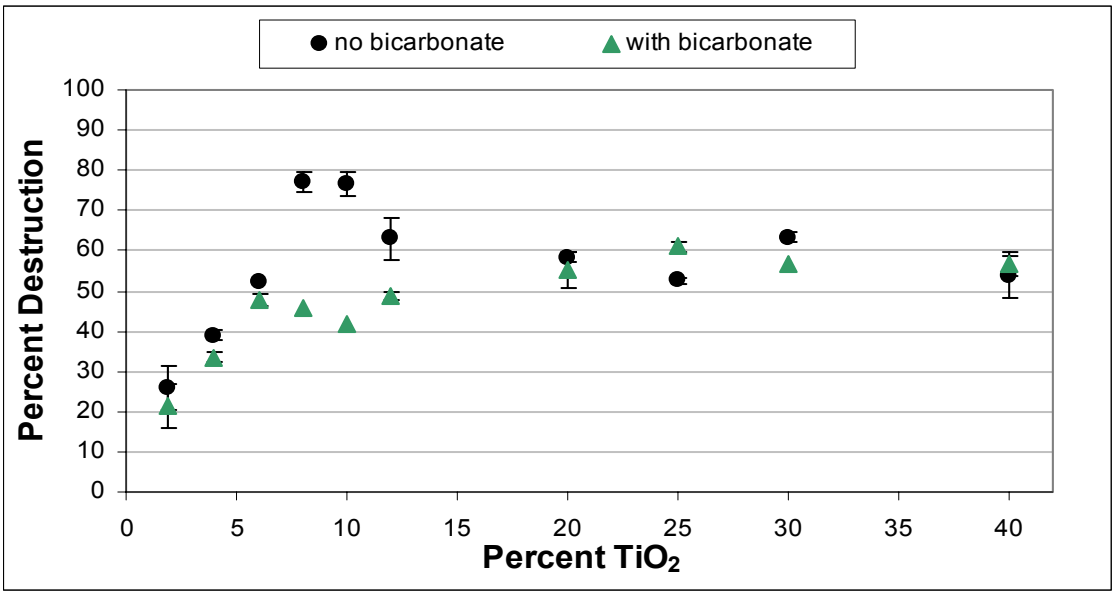

Figure 4-9. Effects of bicarbonate at pH 7.6 versus TiO_2 loading.

It was also thought that surface area may play a role in the leveling-off seen in destruction of RR. As can be seen in Figure 4-10, there is no real trend between BET surface area and titania loading, as well as between pore volume and titania loading. Notice that this surface area is normalized on a volume basis. This trend is different for silica-titania composites prepared by other methods, for which there is a drastic change (up to a loss of 200 m^2/g) in surface area with an increase in percentage of titania (Greiken et al., 2002). In conclusion, there is no correlation between surface area or pore volume and the destruction of RR.

For adsorption studies, CV dye was used because of its cationic nature resulting in a high affinity for the silica-titania composites. These studies were conducted at a low pH (worst case scenario for adsorption of a cation contaminant onto a silica surface). Figure 4-11 compares the amount of adsorption versus titania loading. There is an increase in

adsorption with additional titania in the gel. It is interesting to note, however, that adsorption, similar to the destruction studies, reached a plateau at 12% loading. Therefore, based upon the destruction studies and adsorption studies, an optimal titania loading of 12% TiO_2 was chosen.

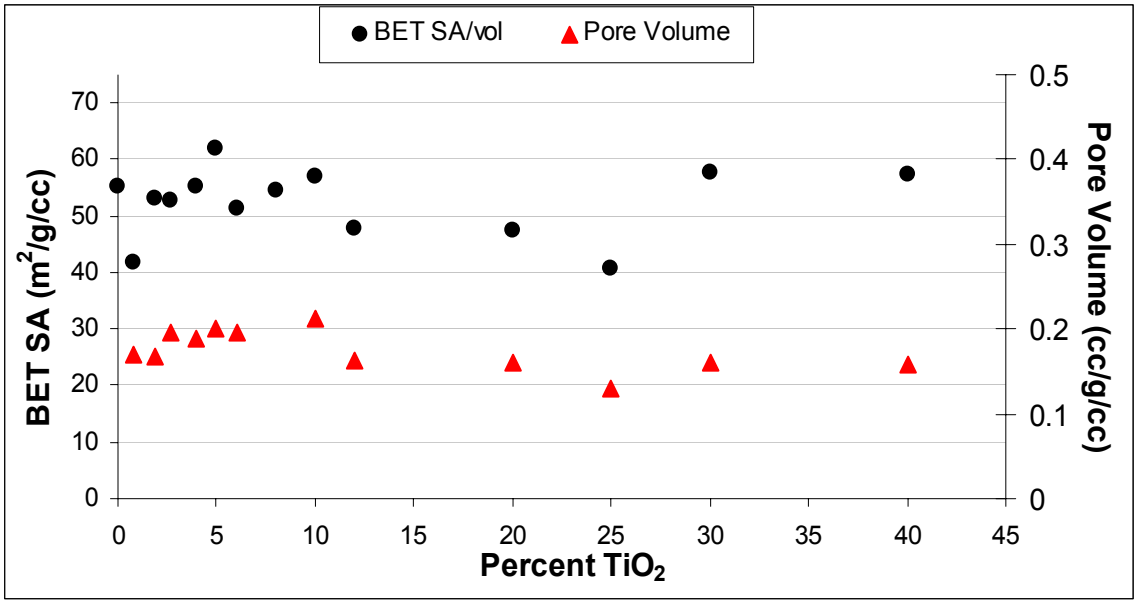

Figure 4-10. BET surface area and pore size versus titania loading.

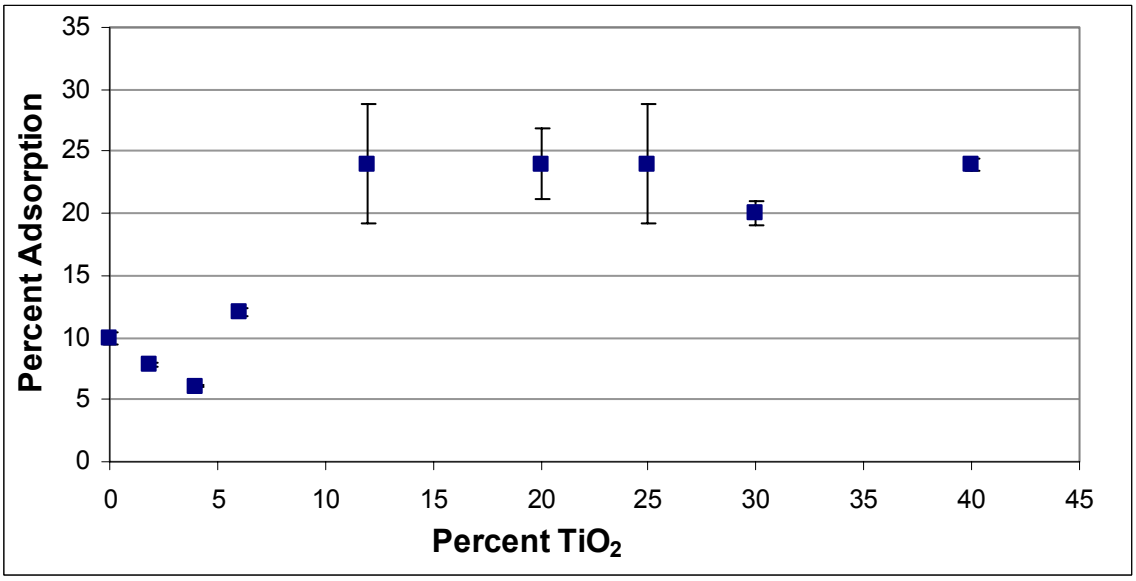

Figure 4-11. Adsorption of CV (10 mg/L) versus TiO_2 loading after 24 hours of mixing.

4.2.2 Curing Temperature

The effect of curing temperature was investigated on gels doped with 6% TiO_2 and those with no TiO_2 (all made with the 140 Å initial formula). The literature showed that there can be an increase in adsorption with gels produced at higher curing temperatures (up to 400°C) due to increasing the ratio of isolated silanols on the surface versus other types of silanols. Yet, the curing temperature may have detrimental effects on the photocatalytic ability of the composites. In looking at the destruction of RR (10 mg/L), Figure 4-12 shows that there is a 30% difference between the 180°C gel versus the 500°C gel at a pH of 7.8. This difference is less pronounced at pH 4. At 800°C, there is a marked decrease in destruction, regardless of pH. This can be explained by both a decrease in surface area of the gels at 800°C (see Figure 4-13) from an average of 275 m^2/g to 150 m^2/g for the titania loaded gel and a phase change of titania.

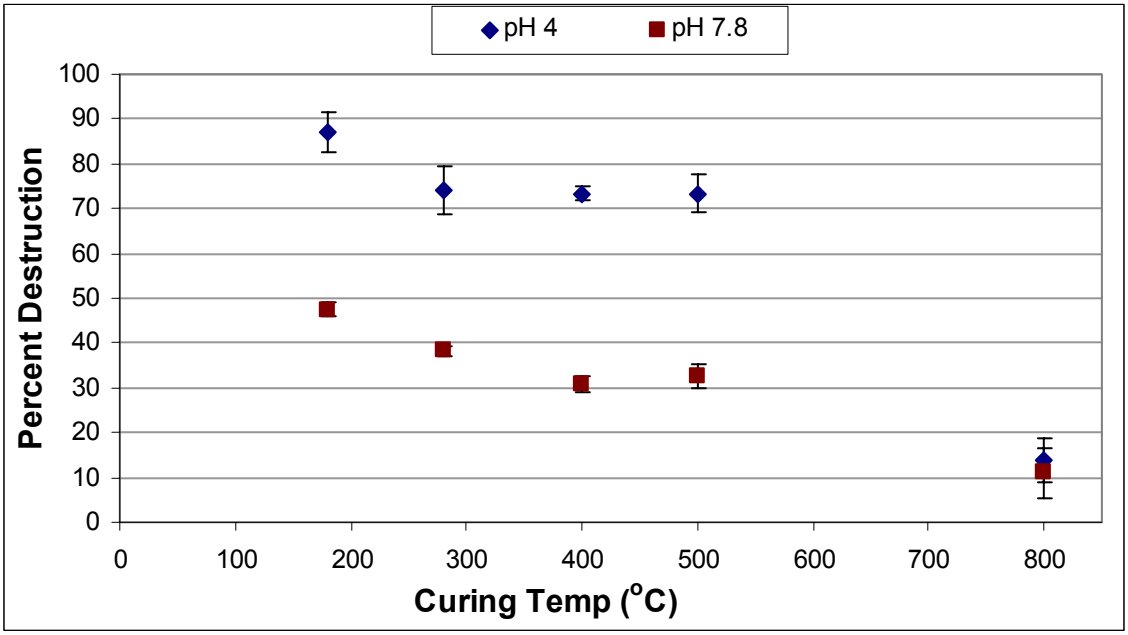

Figure 4-12. Destruction of RR (10 mg/L) after 2 hours UV exposure (0.45 mW/cm^2) versus curing temperature as a function of pH.

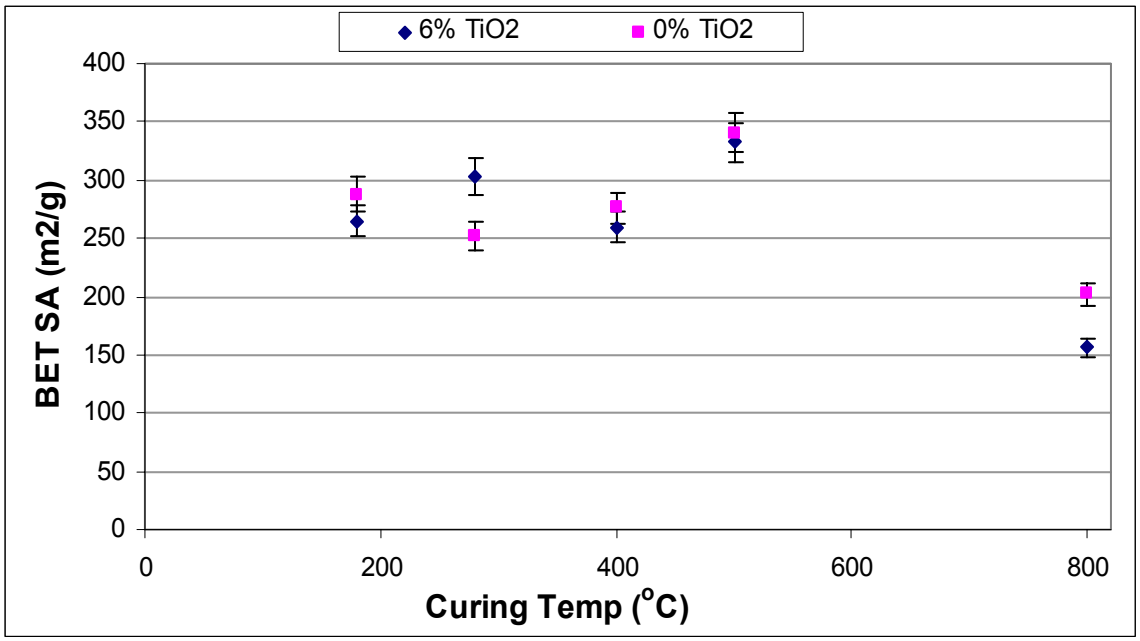

Figure 4-13. Effect of curing temperature on surface area.

The anatase phase of TiO_2 begins transforming into rutile phase at a temperature of 600°C and becomes complete at 1000°C (Zhang et al., 2001). It was thought that the shift in the phase of titania at 800°C may have also affected its photocatalytic ability, but XRD analysis (Figure 4-14) revealed only a slight shift from the anatase phase ($2\theta = 25.3^{o}$) to the rutile phase ($2\theta = 27.4^{o}$) at 800°C which may or may not be enough to have caused a drastic decrease in destruction. It may also be that the phase change is mostly occurring on the surface of the titania where the reactions take place. In other words, the large anatase peak is due to internal anatase crystal formation and the rutile formation is occurring foremost on the surface where it is greatly affecting photocatalysis.

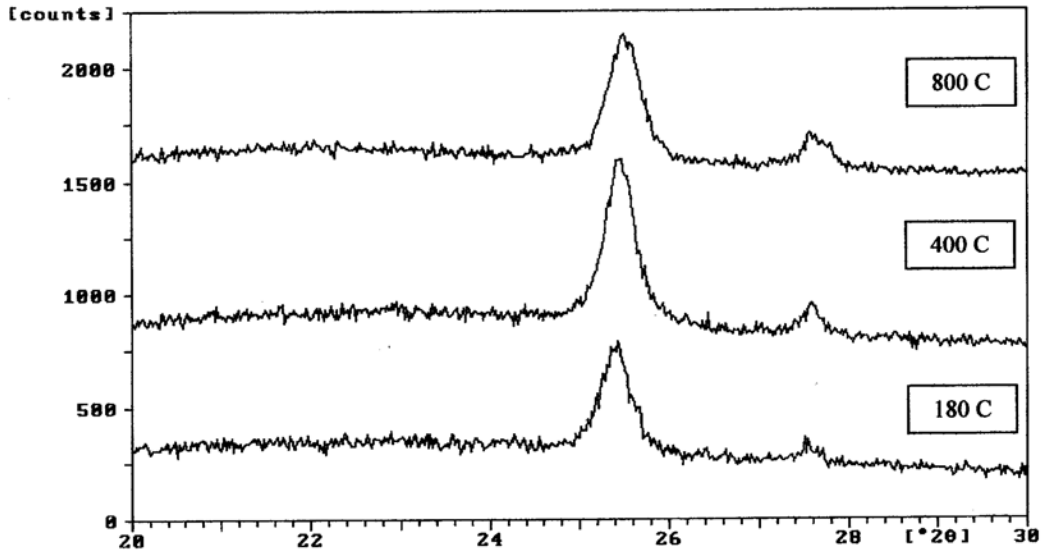

Figure 4-14. XRD analysis of various temperature-cured silica-titania composites.

In looking at adsorption of CV at various curing temperatures, Figure 4-15 shows 800^{o}C with the highest adsorption capacity even though it has the lowest surface area. This may be explained by the cleaner surface (decrease of silanol sights) at this temperature, resulting in the gel displaying a more hydrophobic behavior (Holysz, 1998). This would decrease the competition between water and CV, allowing CV to efficiently interact with the isolated silanols. However, the clean surface can slowly become rehydroxylated when it is in contact with water (Davydov, 2000; Unger et al., 2000). The adsorption ability would then most likely follow the same trend as gels that were treated at lower curing temperatures. Therefore, based upon this and the destruction studies, the optimal curing temperature chosen was 180^{o}C.

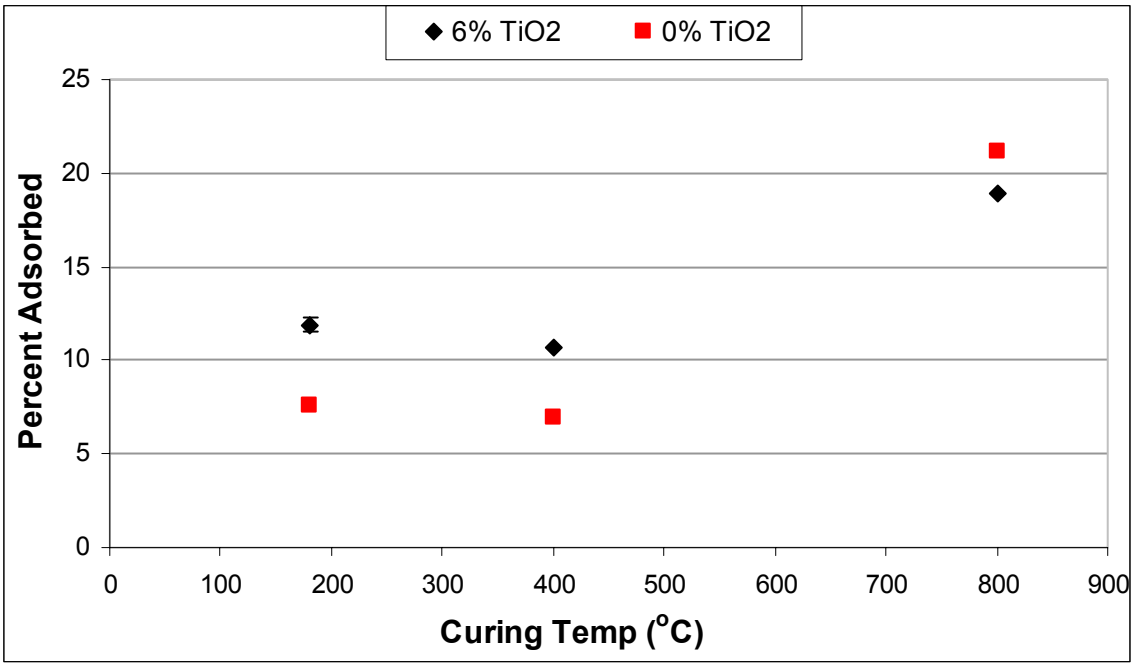

Figure 4-15. Effect of curing temperature on adsorption of CV on gels with and without TiO_2.

4.2.3 Pore Size

Pore size was also investigated for its effects on destruction ability, as well as adsorption ability. Figure 4-16 shows that a large pore size (>140 Å) increases the destruction rates for RR. This is consistent with what is found in the literature. Jung and Park (2000) concluded that high porosity and large pore size facilitate the mass transfer of reactants, such as oxygen and reaction intermediates. Thus, the increase in surface area by small pores is not always effective for high photoactivity. The opposite is true for adsorption, because a smaller pore size results in more surface area available for adsorption. Figure 4-17 shows the largest adsorption with a pore size of 30 Å. Adsorption decreases 73% with larger pores (> 30 Å), and in this range there is no significant difference in adsorption from 60 Å versus 140 Å.

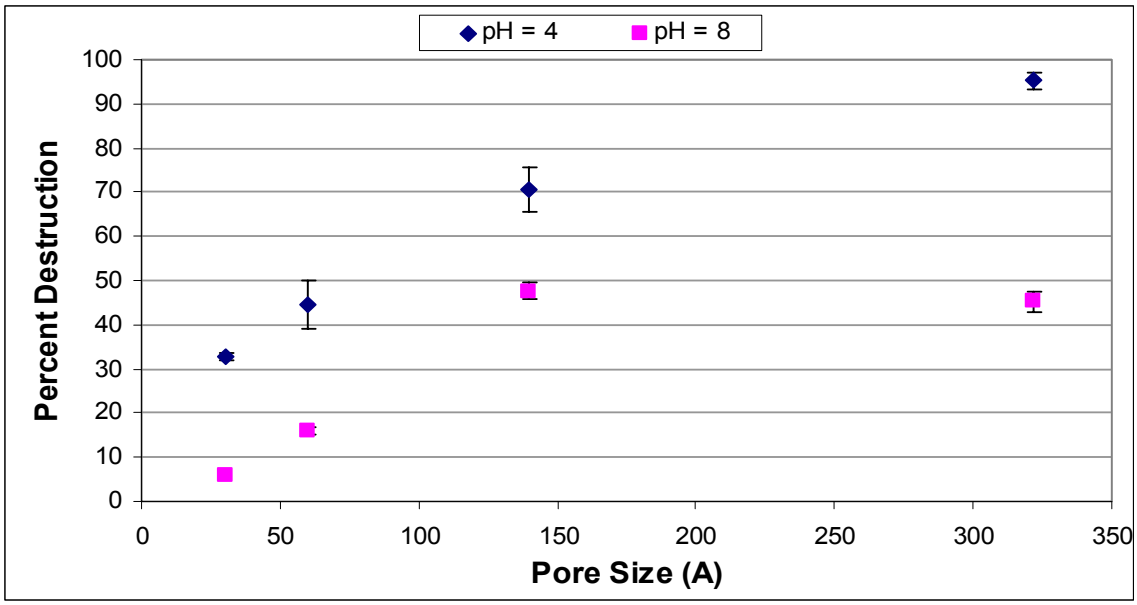

Figure 4-16. Destruction of RR (10 mg/L) after 2 hours UV exposure (0.45 mW/cm^2) versus pore size.

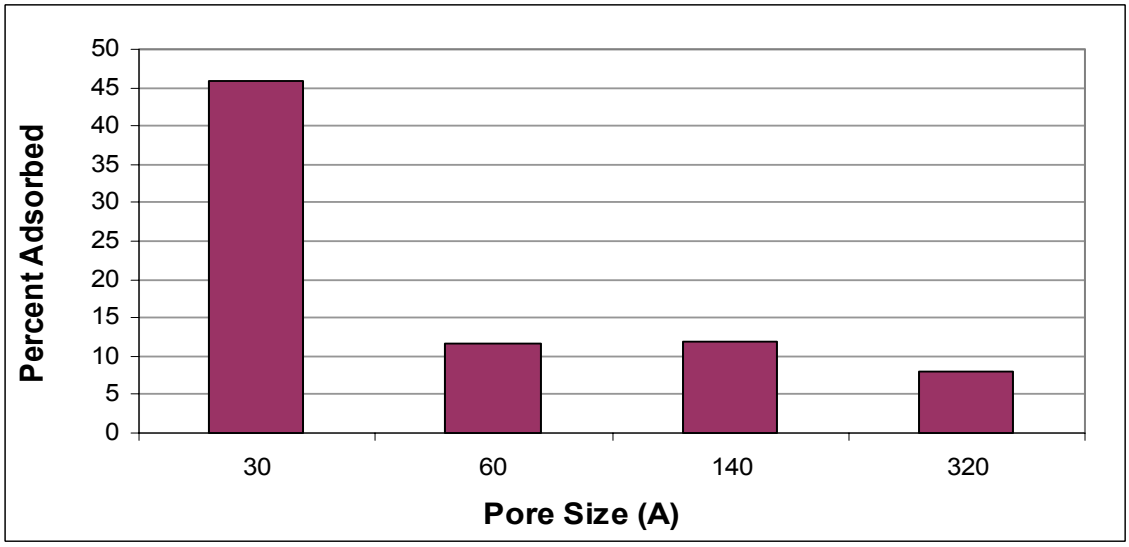

Figure 4-17. Adsorption of CV on gels (6% TiO_2) versus pore size.

4.3 Column Studies

Since the optimal pore size for adsorption is contrary to the optimal pore size for destruction, it was decided to test two pore sizes in a flow-through regenerative column. These studies utilized 12% optimal titania loaded pellets of 30 Å and 140 Å pore sizes. A larger pore size was not analyzed for these studies due to the frailty of the gel at pore

sizes larger than 200 Å. The duplicated column exhaustion curves for each pore size are shown in Figures 4-18 and 4-19. The duplicated runs were done with pellets made from a separate batch.

Table 4-2 summarizes the exhaustion results and shows a longer time to breakthrough of the initial concentration for the column of 30 Å gels. Yet, after the 30 Å pellets reached exhaustion and the system was regenerated by photocatalysis, its level of adsorption ability decreased after each cycle. This was also visually observed. After one hour of UV exposure the 30 Å pellets were still slightly purple, while the 140 Å pellets had regenerated and returned to its initial white state.

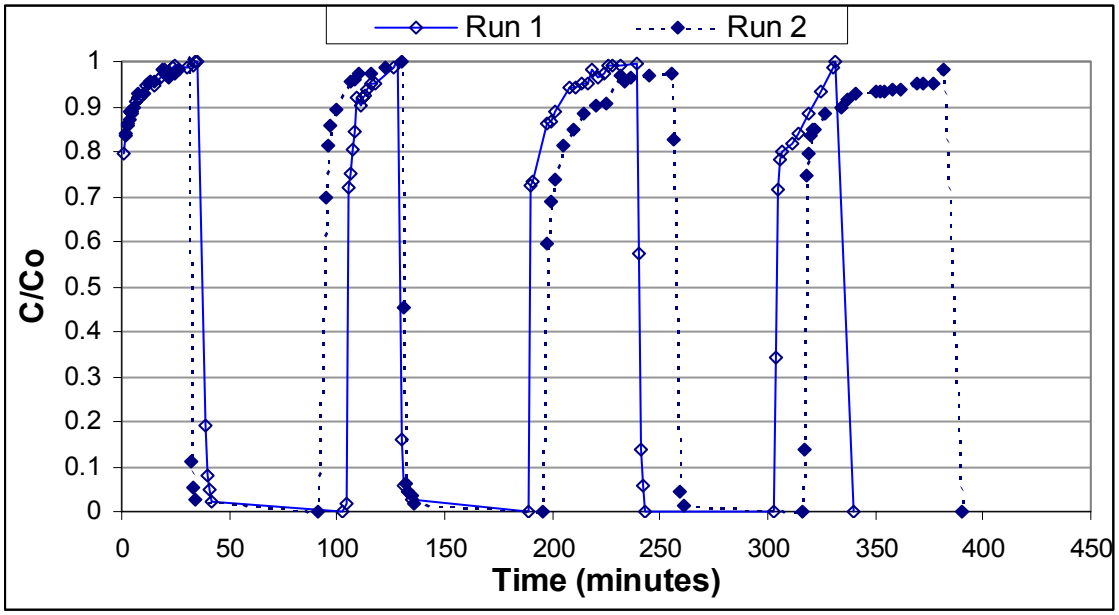

Figure 4-18. Column exhaustion curve for 140 Å pellet (12% TiO_2).

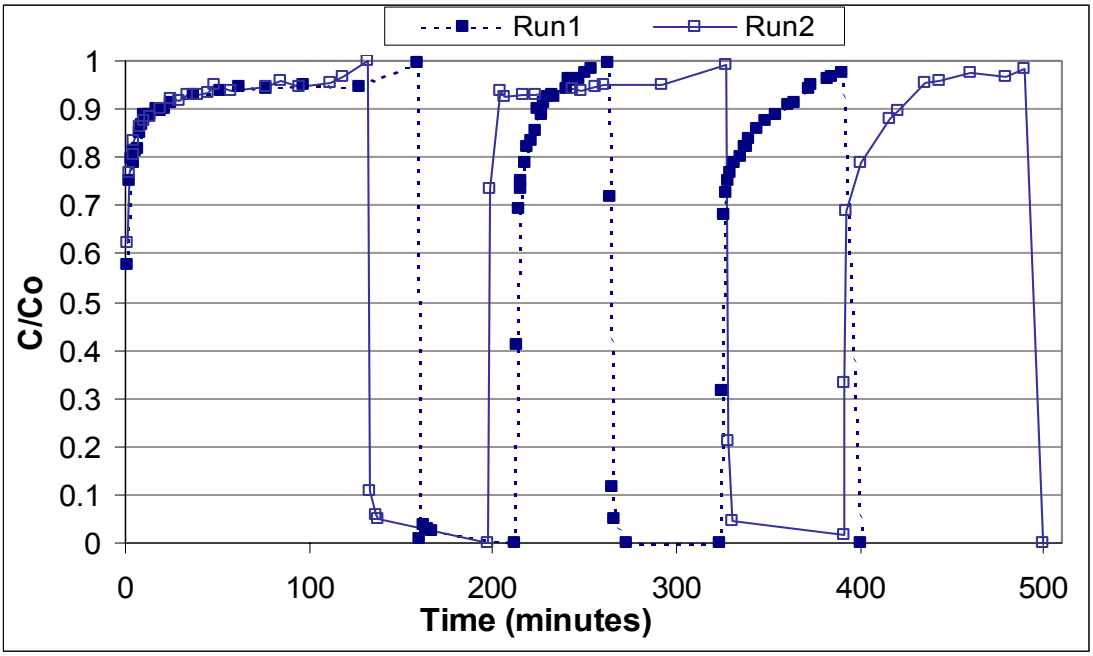

Figure 4-19. Column exhaustion curve for 30 Å pellets (12% TiO_2).

Table 4-2. Exhaustion (C/Co = 1) times (minutes) for column studies.

Pellet Pore Size	140 Å	30 Å
Run 1 Exhaustion Times	36	157
	26	48
	50	64
	27	-
Run 2 Exhaustion Times	28	132
	35	128
	58	98
	65	-
Average Exhaustion Time	40.6	104.5

Both sets of pellets were examined during a column run after exhaustion of the column and it was observed that the 30 Å pellets were still white on the inside, revealing that the total surface available for adsorption was not utilized. The 140 Å pellets were purple throughout their interior, revealing that the available space for adsorption had been exhausted. Thus, the small pore size of the 30 Å gels inhibits the transit of CV solution through the porous matrix. Therefore, the 140 Å sized gels exhibit the greatest efficiency in utilizing its surface area for adsorption and its photocatalytic ability to regenerate.

Thus, the 140 Å pore size was chosen as the optimal pore size for the regenerative system.

In order to determine if a shorter regeneration time was achievable while still keeping the same trend as previously observed, the effect of regeneration time with UV light was examined for the 140 Å column. The time was decreased from 1 hour to 10 minutes and Figure 4-20 shows the comparison of this breakthrough curve with the 1 hour curves. The average breakthrough time was 36 minutes for the 10 minute run versus 46 for the 60 minutes run. Yet, the same trend seems to be exhibited by all 140 Å breakthrough curves. This increase in breakthrough time with each cycle shows the benefit of using the 140 Å pellets, for this trend was not observed with the 30Å pellets.

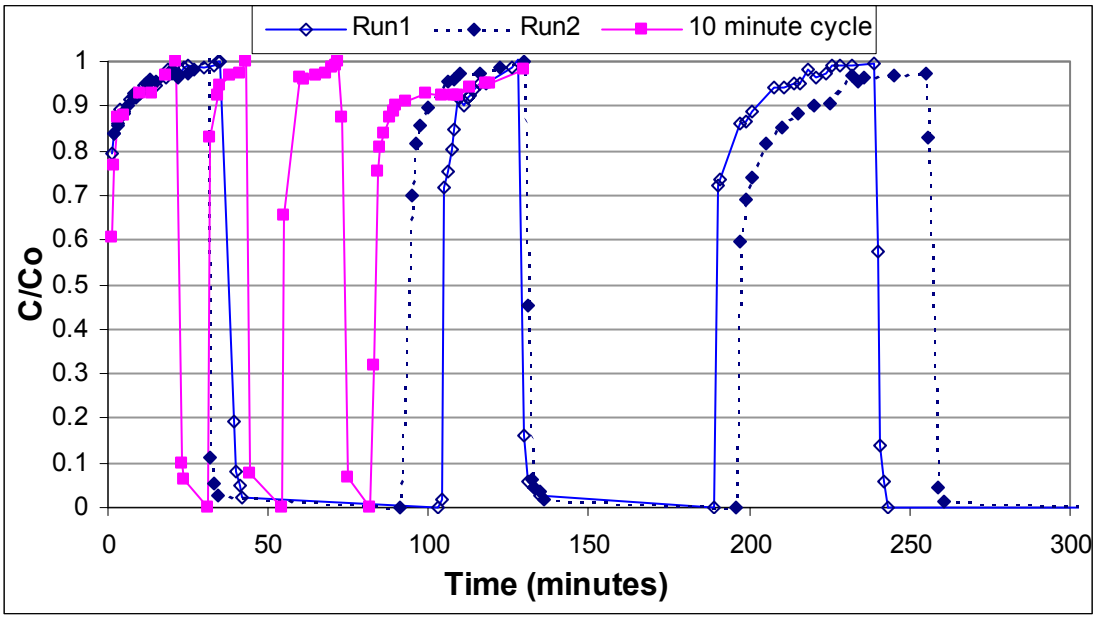

Figure 4-20. Effect of regeneration time on 140 Å column runs.

CHAPTER 5
SUMMARY AND CONCLUSIONS

Silica-titania composites were made using a sol-gel method that allows the doping of titania during gelation. The gelation rate was increased by use of acid catalysts and allowed the composites to be made into pellets with sufficient dispersion of TiO_2 within the silica matrix. Varying the concentration of hydrofluoric acid allowed the manipulation of pore size.

Three variables (TiO_2 loading, curing temperature, and pore size) were investigated to determine the best silica-titania composites for a packed column system. These variables were optimized based upon destruction and adsorption studies and the gels were characterized by surface area and XRD analysis. Reactive red dye (RR) was chosen for its non-photolytic behavior in the analysis of photocatalytic ability for the destruction studies and crystal violet dye was chosen because of its cationic nature for the adsorption studies.

An optimal loading of 12% TiO_2 was chosen based upon the results of studies involving the destruction of RR and adsorption of CV. At higher loadings, it was observed that the titania is agglomerating during mixing, limiting the effective surface area available for reactions on its surface. Also, there was no trend with BET surface area on a volume basis versus titania loading. In addition, the adsorption studies revealed a plateau in uptake beginning at 12% TiO_2.

A curing temperature of 800^{o}C showed the largest effects (a decrease of over 80% destruction) on photocatalytic ability. At this temperature, the surface area decreased and

the phase change of anatase to rutile is evident. This resulted in a dramatic decrease in destruction of RR. Yet, this temperature showed the highest level of adsorption. It was concluded that the clean silica surface and more hydrophobic behavior the silica surface displays at this temperature increased adsorption. This increase in adsorption would decrease over time due to rehydroxylation. The 180^{o}C gel performed the best for destruction and was chosen as the optimal curing temperature.

Concerning pore size, the highest destruction rates were obtained with large pore sizes (> 140 Å). The opposite was true for adsorption, which was greater with small pore sizes (30 Å). Column studies were done in order to determine the best pore size for a regenerative system. The smaller pore size had the longer time to exhaustion, but did not efficiently regenerate. The small pores inhibited the ability of water or the contaminant to move through the matrix, i.e. the path of least resistance was around the pellet versus through the pellet. On the other hand, the 140 Å gels achieved complete regeneration after one hour of UV exposure and efficiently utilized their surface area for adsorption. In conclusion, the optimal pore size chosen for the regenerative flow-through column was 140 Å.

APPENDIX A
COMMON PREPARATION METHODS OF MIXED AND SUPPORTED OXIDES AS DISCUSSED BY GAO AND WACHS (1999).

A.1 Mixed Oxides

A.1.1 Sol-Gel Hydrolysis

Sol-gel hydrolysis involves the acid hydrolysis and condensation of chemically mixed Ti- and Si- alkoxides. In summary, a Ti atom acts as a substitute for a Si atom in the silica network. It is the most widely used method due to its capability in controlling the textural and surface properties of the mixed oxides, but the synthesis conditions can greatly affect the homogeneity of the final product. There is a recently developed two-stage hydrolysis procedure that solves this problem and results in the highest homogeneity. Yet, these mixed oxides can only be obtained at low TiO_2 content, less than 15 wt%. At higher Ti content, due to the larger size of the Ti atom versus Si, atom, there is distortion of the SiO_2 network. This increases the OH content on the silica surface and affects the crystal phase of the TiO_2.

A.1.2 Coprecipitation (Not Used In This Study)

Coprecipitation involves the simultaneous precipitation of SiO_2 and TiO_2 (at high pH) that also includes the formation of linkages with each other. This method also has similar problems to sol-gel hydrolysis.

A.2 Supported Oxides

A.2.1 Impregnation (Not Used In This Study)

Impregnation involves the coating of silica with Ti by mixing with a titanium precursor, such as $TiCl_4$ or a Ti-alkoxide. The following equation summarizes the process:

$$Si - OH + Ti^{+4} \longrightarrow Si - O - Ti$$

The homogeneity of the supported oxide is dependent on the concentration of surface silanols, pretreatment temperature, and molecular size of precursor. A maximum dispersion of TiO_2 was found to be roughly 4.0 Ti atom/nm^2. Consistent creation and determination of the titania phase for catalytic purposes is a major problem with this method.

A.2.2 Chemical Vapor Deposition (not used in this study)

The TiO_2 is deposited onto the porous silica surface from a gaseous metal precursor. Consistent coating is difficult to attain from batch to batch and another problem is the reduction in surface area after coating.

APPENDIX B
DYE STRUCTURES

B.1 Methylene Blue

MW: 319.86

Empirical Formula: $C_{16}H_{18}ClN_3S$

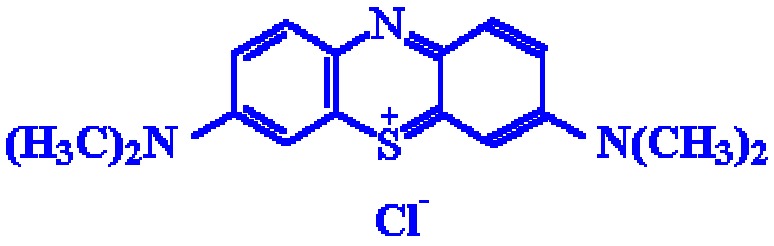

B.2 Malachite Green

MW: 365

Empirical Formula: $C_{23}H_{25}N_2Cl$

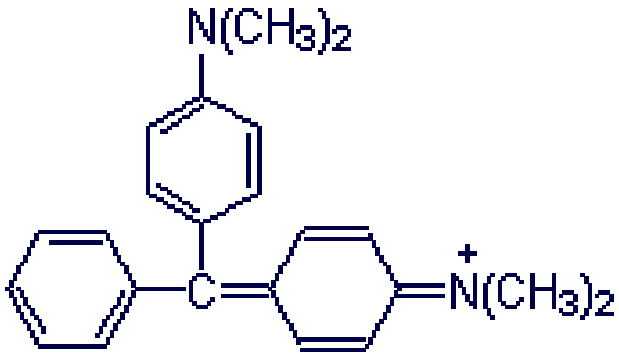

B.3 Crystal Violet

MW: 407.996

Empirical Formula: $C_{25}H_{30}N_3Cl$

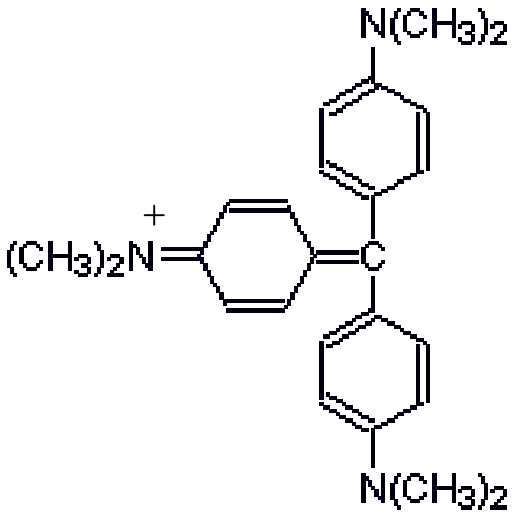

B.4 Reactive Red

MW: 615.34

Empirical Formula: $C_{19}H_{12}Cl_2N_6O_7S_2$

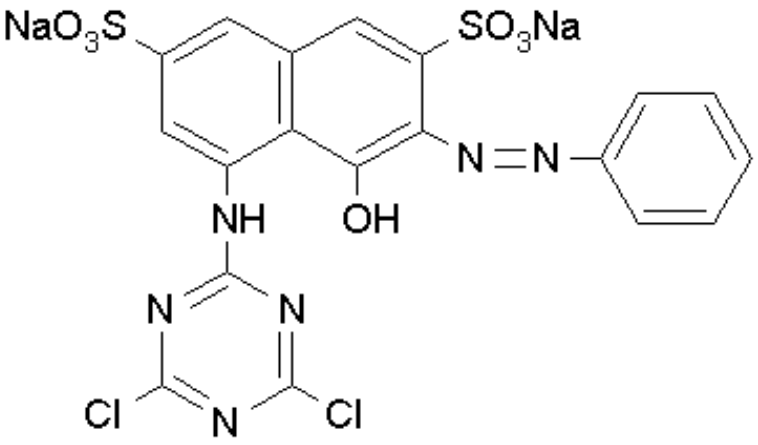

APPENDIX C
TEM AND SEM PICTURES

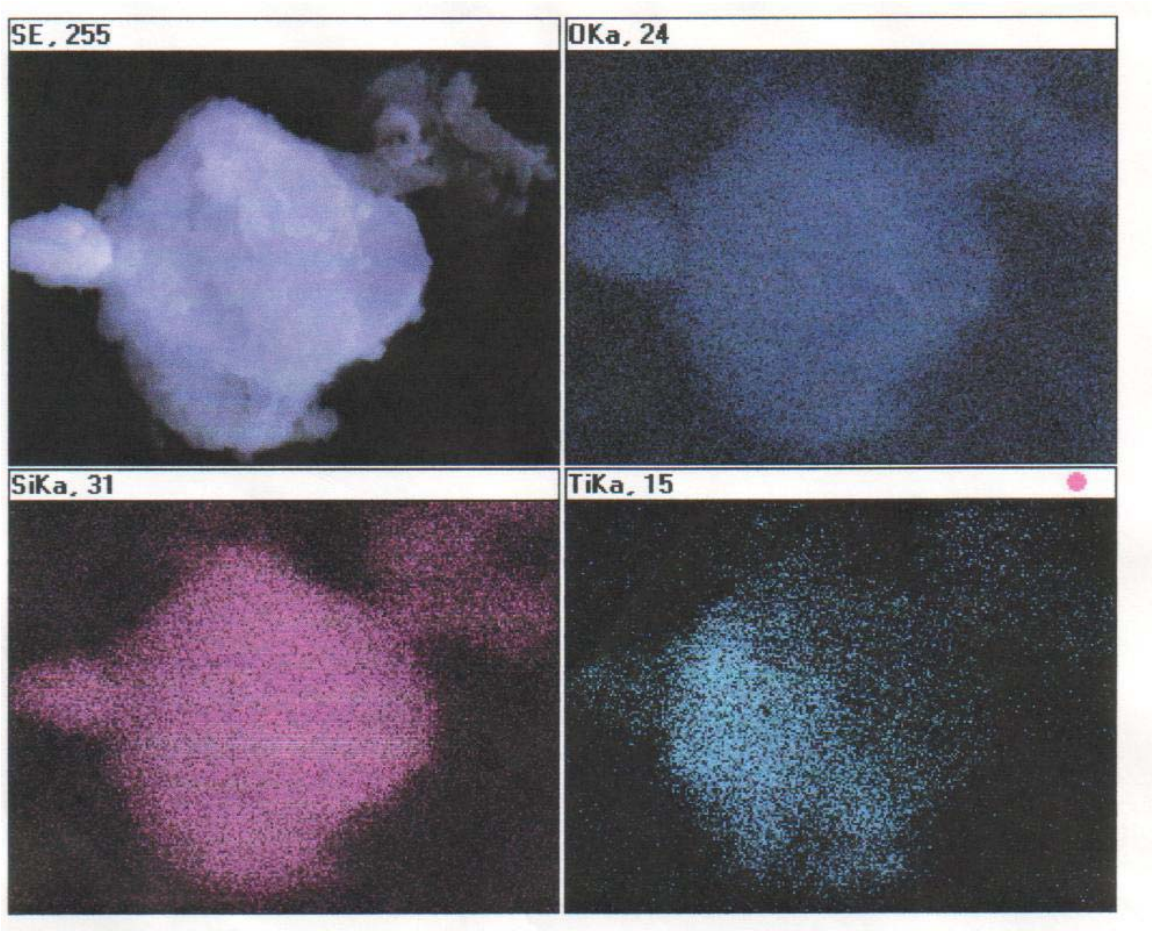

TEM of 4% TiO_2 gel at 20,000x

LIST OF REFERENCES

Abrahams, J., Davidson, S. and Morrison, C., "Optimization of the photocatalytic properties of titanium dioxide," Journal of Photochemistry, Vol. 29, pp. 353-361, 1985.

Al-Ekabi, H. and Serpone, N., "Kinetic studies in heterogeneous photocatalysis: photocatalytic degradation of chlorinated phenols in aerated aqueous solutions over TiO_2 supported on a glass matrix," Journal of Physical Chemistry, Vol. 92, pp. 5726-5731, 1988.

Anderson, C. and Bard, A., "An improved photocatalyst of TiO_2/SiO_2 prepared by a sol-gel synthesis" Journal of Physical Chemistry, Vol. 99, pp. 9882 - 9885, 1995.

Anderson, C. and Bard, A., "Improved photocatalytic activity and characterization of mixed TiO_2/SiO_2 and TiO_2/Al_2O_3 materials," Journal of Physical Chemistry B, Vol. 101, pp. 2611-2616, 1997.

Blake, D., "Bibliography of work on photocatalytic removal of hazardous compounds from water and air," Update Number 1, NREL/TP-473-20300, Golden, CO: National Renewable Energy Laboratory, 1995.

Block, S. and Goswami, D., "Proceedings of ASME Solar Energy Conference," Kohala Coast, Hawaii, pp. 431-438, 1995.

Brinker, C. and Scherer, G., *Sol-Gel Science: The Physics and Chemistry of Sol-Gel Processing*, Academic Press Inc., San Diego, 1990.

Burneau, A. and Gallas, J., "Hydroxyl groups on silica surfaces," in: *The Surface Properties of Silicas*, Legrand, P. (Ed), John Wiley & Sons, Inc., New York, pp. 147-234, 1998.

Chen, H., Zahraa, O. and Bouchy, M., "Inhibition of the adsorption and photocatalytic degradation of an organic contaminant in an aqueous suspension of TiO_2 by inorganic ions," Journal of Physical Chemistry A: Chemistry, Vol. 108, pp. 37-44, 1997.

Chun, H., Yizhong, W. and Hongxiao, T., "Preparation and characterization of surface bond-conjugated TiO_2/SiO_2 and photocatalysis for azo dyes," Applied Catalysis B: Environmental, Vol. 30, pp. 277-285, 2001.

Cox, G., "The influence of silica structure on reversed-phase retention," Journal of Chromatography, Vol. 656, pp. 353-367, 1993.

Crittenden, J., Notthakun, S., Hand, D. and Perram, D., United States Patent 5,182,030, January 26, 1993.

Dabrowski, A., "Adsorption – from theory to practice," Advances in Colloid and Interface Science, Vol. 93, pp. 135-224, 2001.

Davydov, V., "Adsorption on silica surfaces," in: *Adsorption on Silica Surfaces*, Papirer, E. (Ed), John Wiley and Sons Ltd., New York, 2000.

Degussa Technical Bulletin No. 56, "Highly Dispersed Metallic Oxides Produced by the AEROSIL® Process," 1990.

Elizardo, K., "Fighting pollution with hydrogen peroxide," Pollution Engineering, pp. 106-109, September, 1991.

El Shafei, G., "Silica surface chemical properties," in: *Adsorption on Silica Surfaces*, Papirer, E. (Ed), John Wiley and Sons Ltd., New York, pp. 35-62, 2000.

Emeline, A., Ryabchuk, V. and Serpone, N., "Factors affecting the efficiency of a photocatalyzed process in aqueous metal-oxide dispersions: prospect of distinguishing between two kinetic models," Journal of Photochemistry and Photobiology A : Chemistry, Vol. 133, pp. 89-97, 2000.

Environmental Protection Agency, "Best management practices for pollution prevention in the textiles industry," EPA/625/R-96/004, September, 1996.

Environmental Protection Agency, "Sector notebook project – profile of the textile industry part 2," EPA/310-R-97-009, September, 1997.

Gao, X. and Wachs, I., "Titania-silica as catalysts: molecular structural characteristics and physico-chemical properties," Catalysis Today, Vol. 51, pp. 233-254, 1999.

Gerischer, H. and Heller, A., "The role of oxygen in photooxidation of organic molecules on semiconductor particles," Journal of Physical Chemistry, Vol. 95, pp. 5261-5267, 1991.

Goswami, D., Klausner, J., Wyness, P., Martin, A., Mathur, G., Schanze, K., Turchi, C. and Marchand, E., "Solar photocatalytic treatment of groundwater at Tyndall AFB : field test results," University of Florida, LTFNM/SEECL-9302, 1993.

Goworek, J., Nieradka, A. and Dabrowski, A., "Adsorption from ternary mixtures on silica gel of different mesoporosity," Fluid Phase Equilibria, Vol. 136, pp. 333-343, 1997.

Goworek, J., Derylo-Marczewska, A. and Borowka, A., "Adsorption from the liquid phase on silica gels of various structural heterogeneity," Langmuir, Vol. 15, pp. 6103-6106, 1999.

Grabner, G., Li, G., Quint, R., Quint, R. and Getoff, N., "Pulse laser-induced oxidation of phenol in acid aqueous TiO_2," Journal of the Chemical Society Faraday Transactions, Vol. 87, pp. 1097-1101, 1991.

Grieken, R., Aguado, J., Lopez-Munoz, M. and Marugan, J., "Synthesis of size-controlled silica-supported TiO_2 photocatalysts," Journal of Photochemistry and Photobiology A: Chemistry, Vol. 148, pp. 315-322, 2002.

Halmann, M., *Photodegradation of Water Pollutants*, CRC Press, Boca Raton, 1996.

Hanprasopwattana, A., Srinivason, S., Sault, A. and Datye, A., "Titania coatings on monodisperse silica spheres: characterization using 2-propanol dehydration and TEM," Langmuir, Vol. 12, pp. 3173-3179, 1996.

Hench, L. and West, J.," The sol-gel process," Chemical Review, Vol. 90, pp. 33-72, 1990.

Hoffman, M., Martin, S., Choi, W. and Bahnemann, D., "Environmental application of semiconductor photocatalysis," Chemical Reviews, Vol. 95, pp. 69-96, 1995.

Hoigne, J., "Formulation and calibration of environmental reaction kinetics; oxidations by aqueous photooxidants as an example," in: *Aquatic Chemical Kinetics,* Stumm, W. (Ed.), John Wiley & Sons, Inc., New York, pp. 43-70, 1990.

Holysz, L., "The effect of thermal treatment of silica gel on its surface free energy components," Colloids and Surfaces A: Physicochemical and Engineering Aspects, Vol. 134, pp. 321-329, 1998.

Houas, A., Lachheb, H., Ksibi, M., Elaloui, E., Guillard, C. and Hermann, J., "Photocatalytic degradation pathway of methylene blue in water," Applied Catalysis B: Environmental, Vol. 31, pp. 145-157, 2001.

Iler, R., *The Chemistry of Silica*, John Wiley & Sons, New York, 1979.

Jackson, N., Wang, C., Luo, Z., Schwitzgebel, J., Ekert, J., Brock, J. and Heller, A., "Attachment of TiO_2 powders to hollow glass microbeads: activity of the TiO_2-coated beads in the photoassisted oxidation of ethanol to acetaldehyde," Journal of the Electrochemical Society, Vol. 138, pp. 3660-3664, 1991.

Jung, K. and Park, S., "Enhanced photoactivity of silica-embedded titania particles prepares by sol-gel process for the decomposition of trichloroethylene," Applied Catalysis B: Environmental, Vol. 25, pp. 249-256, 2000.

Khan, A., Mazyck, D. and Wu, C., "TiO_2 coated activated carbon: a regenerative technology for water recovery," 021CES-73, International Conference on Environmental Systems, San Antonio, 2002.

Kinniburgh, D. and Jackson, M., "Cation adsorption by hydrous metal oxides and clay," in: *Adsorption of Inorganics at Solid-Liquid Interfaces*, Anderson, M and Rubin, A (Eds.), Ann Arbor Publishers, Ann Arbor, pp. 200-230, 1981.

Legrand, P., "On the silica edge," in: *The Surface Properties of Silicas*, Legrand, P. (Ed), John Wiley & Sons, Inc., New York, pp. 130-200, 1998.

Lei, L., Chu, H., Hu, X. and Yue, P., "Preparation of heterogeneous photocatalysts (TiO_2/alumina) by metallo-organic chemical vapor deposition," Industrial Engineering Chemical Research, Vol. 38, pp. 3381-3385, 1999.

Liu, T. and Cheng, T., "Effects of SiO_2 on the catalytic properties of TiO_2 for the incineration of chloroform," Catalysis Today, Vol. 26, pp. 71-77, 1995.

Lu, M., Chen, J. and Chang, K., "Effect of adsorbents coated with titanium dioxide on the photocatalytic degradation of propoxur," Chemosphere, Vol. 38, pp. 617-627, 1999.

Mao, Y., Schoneich, C. and Asmus, K., "Identification of organic acids and other intermediates in oxidation in oxidation degradation of chlorinated ethanes on TiO_2 surfaces en route to mineralization: a combined photocatalytic and radiation chemical study," Journal of Physical Chemistry, Vol. 95, pp. 10080 – 10089, 1991.

Mao, Y., Schoneich, C. and Asmus, K., "Influence of TiO_2 surface on 1,2-chlorine shift in β-chlorine substituted radicals as studied by radiation chemistry and photocatalysis," Journal of Physical Chemistry, Vol. 96, pp. 8522-8529, 1992.

Mao, Y., Schoneich, C. and Asmus, K., "Radical mediated degradation mechanisms of halogenated organic compounds as studied by photocatalysis at TiO_2 and by radiation chemistry," in: *Photocatalytic Purification and Treatment of Water and Air*, Ollis, D.F. and Al-Ekabi, H. (Eds.), Elsevier Science Publishers, Amsterdam, pp. 49-66, 1993.

Martin, S., Morrison, C. and Hoffman, M., "Photochemical mechanism of size-quantized vanadium-doped TiO_2 particles," Journal of Physical Chemistry, Vol. 98, pp. 13695-13704, 1994.

Matthews, R., "Kinetics of photocatalytic oxidation of organic solutes over titanium dioxide," Journal of Catalysis, Vol. 111, pp. 264-272, 1988.

Mauritz, K., "Sol-gel chemistry," http://www.solgel.com, August 4, 2002.

Millennium Chemical, "Titanium dioxide crystal types," www.millenniumchem.com, November 1, 2002.

Mills, A. and Sawunyama, P., "Photocatalytic degradation of 4-chlorophenol mediated by TiO_2: a comparative study of the activity of laboratory made and commercial TiO_2 samples," Journal of Photochemistry and Photobiology A: Chemistry, Vol. 84, pp. 305-309, 1994.

Nawrocki, J., "The silanol group and its role in liquid chromatography," Journal of Chromatography A, Vol. 779, pp. 29-71, 1997.

NASA, "Requirements definition and design consideration," CTSD-ADV-245, 1998.

Okamoto, K., Yamamoto, Y., Tanaka, H., Tanaka, M. and Itaya, A., "Heterogeneous photocatalytic decomposition of phenol over TiO_2 powder," Bulletin of the Chemical Society of Japan, Vol. 58, pp. 2015-2022, 1985.

Ollis, D., Pelizzetti, E. and Serpone, N., "Destruction of water contaminants," Environmental Science and Technology, Vol. 25, pp. 1523-1529, 1991.

Palmisano, L. and Sclafani, A., "Thermodynamics and kinetics for heterogeneous photocatalytic processes," in: *Heterogeneous Photocatalysis*, Schiavello, M. (Ed), John Wiley & Sons Ltd, New York, pp. 109-132, 1997.

Papirer, E., *Adsorption on Silica Surfaces*, John Wiley and Sons Ltd., New York, 2000.

Persello, J., "Surface and interface structure of silicas," in: *Adsorption on Silica Surfaces*, Papirer, E. (Ed), John Wiley and Sons Ltd., New York, pp. 297-342, 2000.

Powers, K., " The development and characterization of sol gel substrates for chemical and optical applications," Ph.D. Dissertation, University of Florida, 1998.

Sauer, T., Neto, G., Jose, H. and Moreira, R., "Kinetics of photocatalytic degradation of reactive dyes in a TiO_2 slurry reactor," Journal of Photochemistry and Photobiology A: Chemistry, Vol. 149, pp. 47-154, 2002.

Serpone, N., "Brief introductory remarks on heterogeneous photocatalysis," Solar Energy Materials and Solar Cells, Vol. 38, pp. 369-379, 1995.

Serpone, N., Borgarello, E., Harris, R., Cahill, P., Borgarello, M. and Pelizzetti, E., "Photocatalysis over TiO_2 supported on a glass substrate," Solar Energy Materials, Vol. 14, pp. 121-127, 1986.

Sheintuch, M. and Matatov-Meytal, Y., "Comparison of catalytic processes with other regeneration methods of activated carbon," Catalysis Today, Vol. 53, pp. 73-80, 1999.

Sheng, H. and Chi, M., "Treatment of textile waste effluent by ozonation and chemical coagulation," Water Resources, Vol. 27, pp. 1743-1748, 1993.

Suri, R., Liu, J., Hand, D., Crittenden, J., Perram, D. and Mullins, M., "Heterogeneous photocatalytic oxidation of hazardous organic contaminants in water," Water Environment Resources, Vol. 65, pp. 665 – 673, 1993.

Takeda, N., Torimoto, T., Sampath, S., Kuwabata, S. and Yoneyama, H., "Effect of inert supports for titanium dioxide loading on enhancement of photodecomposition rate of gaseous propionaldehyde," Journal of Physical Chemistry, Vol. 99, pp. 9986-9991, 1995.

Tanaka, K., Capule, M. and Hisanaga, T., "Effect of crystallinity of TiO_2 on its photocatalytic action," Chemical Physics Letters, Vol. 187, pp. 73-76, 1991.

Torimoto, T., Ito, S., Kuwabata, S. and Yoneyama, H., "Effects of adsorbents used as supports for titanium dioxide loading photocatalytic degradation of propyzamide," Environmental Science and Technology, Vol. 30, pp. 1275-1281, 1996.

Turchi, C. and Ollis, D., "Photocatalytic degradation of organic water contaminant: mechanisms involving hydroxyl radical attack," Journal of Catalysis**,** Vol. 122, pp. 178-192, 1990.

Uchida, H., Itoh, S. and Yoneyama, H., " Photocatalytic decomposition of propyzamide using TiO_2 supported on activated carbon," Chemistry Letters, pp. 1995-1998, 1993.

Unger, K., *Porous Silica,* Elsevier, 1979.

Unger, K.,Kumar, D., Ehwald, V. and Grossman, F., "Adsorption on silcia surfaces from solution and its impact on chromatographic separation techniques," in: *Adsorption on Silica Surfaces*, Papirer, E. (Ed), John Wiley and Sons Ltd., New York, pp. 565-594, 2000.

US Geological Survey Minerals Information, "Titanium statistical compendium," http://minerals.usgs.gov/minerals/pubs/commodity/titanium/stat/, August 1, 2002.

Voinov, M. and Augustynski, J., "Introduction to the physics of semiconductor photocatalysts," in*: Heterogeneous Photocatalysis*, Schiavello, M. (Ed.), John Wiley & Sons Ltd., New York, pp. 1-34, 1997.

Wu, T., Liu, G., Zhao, J., Hidaka, H. and Serpone, N., "Evidence for H_2O_2 generation during the TiO_2 assisted photodegradation of dyes in aqueous dispersions under visible light illumination," Journal of Physical Chemistry B, Vol. 103, pp. 4862-4867, 1999.

Yamazaki, S., Matsunaga, S. and Hori, K., "Photocatalytic degradation of trichloroethylene in water using TiO_2 pellets," Water Resources, Vol. 35, pp. 1022-1028, 2001.

Yoneyama, H. and Torimoto, T., "Titanium dioxide/adsorbent hybrid photocatalysts for photodestruction of organic substances of dilute concentrations," Catalysis Today, Vol. 58, pp. 133-140, 2000.

Zhang, Y., Crittenden, J., Hand, D. and Perram, D., "Fixed-bed photocatalysts for solar decontamination of water," Environmental Science and Technology, Vol. 28, pp. 435-442, 1994.

Zhang, Y., Weidenkaff, A. and Reller, A., "Mesoporous structure and phase transition of nanocrystalline TiO_2," Materials Letters, Vol. 3429, 2001.

BIOGRAPHICAL SKETCH

Danielle Julia Eller Londeree was born in June of 1979 in Deerfield Beach, Florida. Her dad graduated from UF with an agricultural engineering degree and took over the family business of manufacturing large-scale water pumps. Her brothers also graduated from UF and followed in his footsteps, both receiving engineering degrees and working for the family business. Their encouragement is what made Danielle want to be an engineer, and following high school graduation from Zion Lutheran Christian School in 1997, she pursued an engineering degree from UF. After getting married to Donald Londeree in August of 2001, she received her B.S. in Environmental Engineering in December of 2001. Then her thirst for knowledge and her desire to contribute to the family business led her to pursue graduate school, focusing on water quality. In the future, she hopes to use the knowledge that she has obtained in graduate school to increase the scope of the family business and assist in solving the world's water problems, on both a quantity and quality level.